Monthly Notices
of the
ROYAL ASTRONOMICAL SOCIETY
MNRAS **464,** 1607–1632 (2017) doi:10.1093/mnras/stw2432

Merging white dwarfs and Type Ia supernovae

L. R. Yungelson[1]★ and A. G. Kuranov[2]

[1]*Institute of Astronomy of the Russian Academy of Sciences, 48 Pyatnitskaya Str., Moscow, Russia*
[2]*Sternberg Astronomical Institute, Moscow M.V. Lomonosov State University, Moscow, Russia*

Accepted 2016 September 22. Received 2016 September 20; in original form 2016 July 25

ABSTRACT

Using population synthesis, we study a double-degenerate (DD) scenario for Type Ia supernovae (SNe Ia), aiming to estimate the maximum possible contribution to the rate of SNe from this scenario and the dependence of the delay-time distribution (DTD) on it. We make an extreme assumption that all mergers of super-Chandrasekhar pairs of CO white dwarfs (WDs) and mergers of CO WDs more massive than 0.47 $M_{\odot}$ with hybrid or helium WDs more massive than 0.37 $M_{\odot}$ produce SNe Ia. The models are parametrized by the product of the common envelope efficiency and the parameter of binding energy of stellar envelopes, $\alpha_{\rm ce}\,\lambda$, which we vary between 0.25 and 2. The best agreement with observations is obtained for $\alpha_{\rm ce}\,\lambda = 2$. A substantial contribution to the rate of SNe Ia is provided by the pairs with a hybrid WD. The estimated Galactic rate of SNe Ia is 6.5×10^{-3} yr^{-1} (for the mass of the bulge and thin disc equal to 7.2×10^{10} M$_{\odot}$), which is comparable to the observational estimate $(5.4 \pm 0.12) \times 10^{-3}$ yr^{-1}. The model DTD for $1 \leq t \leq 8$ Gyr satisfactorily fits the DTD for SNe Ia in the field galaxies (Maoz, Mannucci & Brandt). For this epoch, the model DTD is $\propto t^{-1.64}$. At earlier and later epochs, our DTD has a deficit of events, as in other studies. Marginal agreement with the observational DTD is achieved even if only CO+CO WDs with $M_1 \geq 0.8\,{\rm M}_{\odot}$ and $M_2 \geq 0.6\,{\rm M}_{\odot}$ produce SNe Ia. A better agreement of observed and modelled DTD may be obtained if tidal effects are weaker than assumed and/or the metallicity of the population is much lower than solar.

Key words: binaries: close – supernovae: general.

1 INTRODUCTION

The exceptional role of Type Ia supernovae (SNe Ia) in explorations of the riddles of the Universe is a result primarily of the fact that, with certain caveats, these objects can be considered as 'standard candles' and serve as a measure of cosmic distance. The nature of SNe Ia is still, however, elusive. There exists only an agreement that they are related to the thermonuclear explosions of white dwarfs (WDs) (Hoyle & Fowler 1960).

The evolution of close binaries leading to the formation of potential precursors of SNe Ia has been discussed for more than 45 years, starting with the papers by Tutukov & Yungelson (1979b), Webbink (1979), Tutukov & Yungelson (1981), Iben & Tutukov (1984) and Webbink (1984). The current status of the problem is considered in the recent reviews by, for example, Hillebrandt et al. (2013), Maoz, Mannucci & Nelemans (2014), Postnov & Yungelson (2014) and Ruiz-Lapuente (2014).

There are two main competing hypothetical scenarios for the evolution of close binaries to SNe Ia: (a) the 'single-degenerate' model (SD), implying the explosion of a CO WD that accumulated matter from a non-degenerate donor; and (b) the 'double-degenerate' model (DD), in which the SN Ia is a result of the merger of a pair of WDs. Other scenarios, such as a merger of WD with the core of a red giant (core-degenerate one in modern terms), (Sparks & Stecher 1974; Ilkov & Soker 2012) or direct collisions of WDs (Raskin et al. 2009; Rosswog et al. 2009b) usually considered to be less important. We do not consider SNe Ia induced by tidal interactions of WDs with black holes (Rosswog, Ramirez-Ruiz & Hix 2009a) and 'resonant' ones (McKernan & Ford 2016), as well as the possible enhancement of SNe Ia rate owing to dynamical interactions in stellar clusters (Shara & Hurley 2002).

The topic of the present paper is the double-degenerate scenario. Its main assumption is that the loss of angular momentum via gravitational wave radiation by a close binary with WD components reduces the separation of the WDs and leads to Roche lobe overflow (RLOF) by the lower-mass one (with the larger radius). Early simple analytical estimates using the mass–radius relationship (Tutukov & Yungelson 1979b) suggested that for a mass-ratio of components $\gtrsim 2/3$, the WD is unstable and the latter completely disrupts, presumably on a time-scale comparable to the orbital period of the system $P_{\rm orb}$, forming a disc that gradually settles onto the WD. Components of the binary thus 'merge'. Later, Nelemans

★ E-mail: lev.yungelson@gmail.com

et al. (2001b) and Marsh, Nelemans & Steeghs (2004) showed that the stability of mass loss depends also on the efficiency of the tidal interaction in the binary. Smoothed particle hydrodynamics (SPH)-calculations taking into account the physical equation of state demonstrated that the WD disrupts in $\sim 100 P_{\rm orb}$ and merger occurs in the direct impact regime (e.g. D'Souza et al. 2006; Dan, Rosswog & Brüggen 2009; Dan et al. 2011). While the early versions of the scenario assumed as precursors of SN Ia only pairs of CO WDs with $M_1 + M_2 \geq M_{\rm Ch}$ (Tutukov & Yungelson 1979a; Webbink 1979; Tutukov & Yungelson 1981; Webbink 1984; Iben & Tutukov 1984), currently mergers of sub-$M_{\rm Ch}$ systems with CO accretors and CO, He and hybrid donors[1] are being considered too. The evidence for the necessity of considering sub-$M_{\rm Ch}$ SNe Ia has been summarized by van Kerkwijk, Chang & Justham (2010).

However, an important problem that is apparently unresolvable in the foreseeable future is that the disruption of the donor and the formation of a quasi-steady configuration are modelled by SPH-methods, with a resolution of $\sim 10^7$ cm at best, while models of nuclear burning deal with scales down to ~ 1 cm. SPH-computations allow us only to determine whether the necessary condition of detonation – an energy release time-scale $\tau_{3\alpha}$ shorter than the local dynamical time-scale $\tau_{\rm dyn}$ – is fulfilled, while the necessary and sufficient condition for self-sustained detonation is the supersonic speed of flame propagation. If it does not follow immediately from the computations of merger that the latter condition is fulfilled, one has to judge whether detonation is possible, using the results from SPH-calculations as an input for mesh-based codes of various degrees of sophistication. The aim is to determine whether the formation of 'hot spots' in the merger products is possible; that is, to calculate the critical sizes of hot regions that ignite and yield propagating detonations. The parameters of hot spots (density, temperature and its gradient, geometry) for He were found using 1D calculations by Holcomb et al. (2013) and Shen & Moore (2014), and for a C/O mixture most recently by Seitenzahl et al. (2009) and Shen & Bildsten (2014).[2]

The above circumstance makes the real role of the DD-channel in the production of SNe Ia uncertain. The aim of the present study is to estimate the possible contribution of the DD scenario to the rate of SNe Ia and the dependence of the delay-time distribution for SNe Ia in this scenario under an *extreme assumption that all mergers of super-Chandrasekhar CO+CO pairs of WDs as well as mergers of CO WDs and massive He and hybrid WDs result in SNe Ia*.

In Section 2 we briefly review the extant results of merger computations and show that they are still inconclusive. For this reason, we compute the total rate of mergers of WD pairs with He, hybrid and CO donors and CO or ONe accretors for various parameters of population synthesis, aiming to estimate the upper limit of the contribution of mergers to the SNe Ia rate and, particularly, of different pairs to the latter. In Section 3 we present the assumptions we use. In Section 4 we present our results. This is followed by a discussion in Section 5 and the conclusions in Section 6. Some additional information is provided in the Appendix.

[1] $M \simeq (0.32–0.60)\,{\rm M}_\odot$ CO WDs that descend from He stars have mass abundances of He up to almost 90 per cent in the $\simeq$(0.20–0.01) $\rm M_\odot$ envelopes; more massive post-He-star WDs have only traces of He in their envelopes.

[2] Such a method may lead to the smoothing of the temperature distribution and a distortion of the distribution of chemical species, potentially influencing the results of the calculations; see, for example, the detailed discussions by Shen & Moore (2014) and Katz et al. (2016). Another important factor is the sophistication of the nuclear reactions grid.

2 MERGER COMPUTATIONS

The merger of WDs can proceed through several stages: (i) disruption of the less-massive WD and dynamical accretion; (ii) relaxation of the resulting configuration to the quasi-steady state; (iii) evolution of the merger product to a SN or an accretion-induced collapse (AIC).

Merger products have a similar structure (Guerrero, García-Berro & Isern 2004): a cold virtually isothermal core, a pressure-supported envelope, a Keplerian disc, and a tidal tail. If explosion does not happen during the dynamical stage of merger, the He or C/O mixture may explode in the envelope, which is the hottest part of the object. The detonation of He in the envelope may lead to the detonation of C at the periphery of the accretor ('edge-lit detonation') or in its central region, which is compressed by converging shocks ('double-detonation'). The explosion of a CO WD results in its complete disruption. While the major fraction of the accretor mass burns to radioactive Ni, which determines the optical luminosity and spectrum of the SN Ia, the donor burns to intermediate-mass elements, which are responsible for observational manifestations of SN Ia at maximum brightness (Shigeyama et al. 1992; Sim et al. 2010). Thus, the main role of the donor explosion (or of its remnants after disruption) is to trigger the detonation of the accretor (Rosswog et al. 2009b).

The sub-$M_{\rm Ch}$ DD scenario is to a significant extent related to the still hypothetical 'double-detonation' scenario with a He-rich donor, either degenerate or non-degenerate; see, for example, Livne & Glasner (1991); Shen & Bildsten (2014). Sim et al. (2010), based on a series of 1D calculations of pure detonations of CO WDs with post-processing nucleosynthesis and radiation transfer, concluded that sub-$M_{\rm Ch}$ explosions are a viable model for SNe Ia for *any* evolutionary scenario leading to explosions in which the optical display is dominated by the material produced in the detonation of the primary WD.

Systematic studies of mergers of WD pairs with He WDs or CO/He hybrid WD donors and CO WD accretors with mass from 0.4 $\rm M_\odot$ to 1.2 $\rm M_\odot$ were performed by Guillochon et al. (2010) and Dan et al. (2012, 2014), using grid-based and SPH-codes, respectively. They found that for He/hybrid+CO pairs of WDs, the condition $\tau_{3\alpha} \leq \tau_{\rm dyn}$ is fulfilled prior to merger or at the surface contact provided that $M_{\rm CO} \leq 1.1$ $\rm M_\odot$ and that the mass of the He-rich donor $\gtrsim$0.4 $\rm M_\odot$. In some cases, detonation is caused by instabilities in the accretion stream. It remains unclear, however, whether these surface detonations may initiate detonation in the core. For CO+CO WD pairs, dynamical burning conditions were met for $(M_1 + M_2) \geq$ 2.1 $\rm M_\odot$ only.

Pakmor et al. (2010, 2012) studied 'violent' (see below) mergers of several pairs of equal and almost equal mass CO WDs ($M_1 =$ 0.9 $\rm M_\odot$) in which they *assumed*, based on computations by Seitenzahl et al. (2009), that a detonation occurs if, during compression and heating of the matter encountering the accretor, the threshold $T \geq 2.5 \times 10^9$ K at a density of about 2×10^6 g cm^{-3} is reached. As a critical mass ratio for detonation, Pakmor et al. inferred $M_2/M_1 =$ 0.8. Bearing in mind that traces of He of (10^{-3}–10^{-2}) $\rm M_\odot$ should be present at the surface of all CO WDs and that He is ignited more readily than carbon and, thus, may facilitate nuclear ignition during the merger (Guillochon et al. 2010), and based on the computation of a merger of 1.1 $\rm M_\odot$ and 0.9 $\rm M_\odot$ WDs with 0.01-$\rm M_\odot$ He envelopes, Pakmor et al. (2013) speculated that He-ignited (CO+CO) WD and (CO+He) WD mergers may present a unified model for normal and rapidly declining SNe Ia. The model does not explain SNe Ia with strongly mixed ejecta (SN 2002cx-type ones).

Ruiter et al. (2013) used the relationship between the accretor mass and M_{bol} at maximum for detonating sub-M_{Ch} mass CO WDs to construct the brightness distribution expected for violent mergers of pairs of CO WDs by population synthesis. Under certain assumptions, the shape of the brightness amplitude distribution matches the observations well. However, the model needs further elaboration in respect of nuclear display and spectral features. At present, the model encounters serious difficulties in reproducing spectrophotometric features of SNe Ia because of asymmetries in the distribution of ejecta (Bulla et al. 2016).

Dan et al. (2015) analysed the possibility of post-merger explosions for some previously found configurations, using them as an input for the grid-based 2D hydrodynamical calculations with rotation by the code FLASH (Fryxell et al. 2000; Dubey et al. 2009). It was found that *immediately* after completion of merger, detonation does not occur in either He+CO or CO+CO pairs, because of too low a density in the hot regions (envelopes). A similar conclusion for CO+CO pairs was reached by Zhu et al. (2013), Tanikawa et al. (2015) and Sato et al. (2015). However, it was suggested that an insufficient resolution in most computations, $\lesssim 500k$ ($k = 1024$ particles per $M_\odot$), may be the reason for this (Sato et al. 2016). In test computations with resolutions up to $\approx 2000k$ in which the $^{12}C + {}^{12}C$ reaction was also taken into account, the detonation conditions of Seitenzahl et al. (2009) were met by pairs of WD with $M_1 \gtrsim 0.8\,M_\odot$ and

$$M_2/M_1 \gtrsim 0.8\,(M_1/M_\odot)^{-0.84}. \quad (1)$$

It may be expected that a further increase of resolution will enable to resolve smaller hot regions. Sato et al. (2016) also noted that the study of possible mergers at contact for He+CO pairs needs a higher resolution, because the occurrence of helium detonation depends strongly on the mass of the helium layer. This may affect the 'unified' model of Pakmor et al. (2013).

Dan et al. (2015) found that the criteria for spontaneous detonation discovered by Holcomb et al. (2013), Shen and Moore (2014), Seitenzahl et al. (2009) may be met during the evolution of merger products in their most dense and hot regions. However, because of the above-mentioned discontinuity in the resolution of SPH and mesh-based computations, hot spots were located 'manually', assuming that the merger products evolved to conditions necessary for detonation. It was found that He detonation may or may not lead to detonation in the centre. In addition, it was found that the initial perturbation may not initiate detonation in the envelope, but converging shocks may cause detonation in the core. Some post-merger configurations do not lead to SN Ia.[3]

Raskin et al. (2012), who also computed the merger of WDs by SPH, have shown that in the models of mergers of CO WDs with He envelopes ($M_{1,2} = (0.64\text{–}1.06)\ M_\odot$, $M_{He} = (0.013\text{–}0.015)\ M_\odot$), He detonates in the merger process, but the released energy is not sufficient to initiate detonation in the core of the merger product. In a continuation of this study, Moll et al. (2014) analysed the possibility of detonation using a grid-based code with a higher resolution and showed that secondary detonation is possible, if massive ($M_{1,2} \geq 1.06\ M_\odot$) WDs merge. Note, however, that, as in the studies of Pakmor et al. (2010, 2012, 2013), these computations rely on an artificial ignition of detonation.

[3] A caveat should be inserted that the results of Dan et al. (2014, 2015) may be influenced by the assumption that their initial models of CO WDs with masses 0.45 $M_\odot$ to 0.6 $M_\odot$ have a 0.1 $M_\odot$ He mantle; such an abundance may be an overestimate (Iben & Tutukov 1985; Chen & Han 2002).

The long-term post-merger evolution of the merger product of CO WDs that avoided detonation at the merger itself was simulated by Shen et al. (2012) and Schwab, Quataert & Kasen (2016) using the α-viscosity prescription. Schwab et al. (2012) performed a similar study for a He+CO WD merger. It was found that merger products evolve on the viscous time-scale towards spherical configurations. A hot, slowly rotating and radially extended envelope forms. Certain amount of mass may be lost by the stellar wind. At the end of this stage, owing to dynamical and viscous heating, the temperature at the base of the envelope may become high enough for off-centre burning. In the case of He/CO mergers, it is possible that He-detonation ensues and a SN Ia explodes. As argued by Schwab et al. (2016) on the basis of 1D computations, in the case of CO WDs, if the mass of the object remains below $1.35\,M_\odot$, the inward propagation of the burning leads to the formation of a massive ONe WD. In merger remnants with a higher mass, neon ignites off-centre. It is expected that a silicon WD forms. If the mass remains super-M_{Ch}, further nuclear evolution will result in the formation of an iron core and collapse, producing a neutron star. The optical manifestation of an accompanying SN is uncertain. In fact, the study of Schwab et al. questions the role of mergers of CO WDs with mass below $\approx 2\ M_\odot$ as progenitors of SNe Ia in the DD-scenario.

Ji et al. (2013) have shown (in 2D) that the merger of a pair of (0.6+0.6) $M_\odot$ CO WDs produces a rapidly rotating WD surrounded by a hot corona and a thick, differentially rotating disc, which is strongly susceptible to the magneto-rotational instability. Instability leads to the rapid growth of the initially dynamically weak magnetic field in the disc, to spin-down of the 'new-born' WD, and to the central ignition of the latter. However, as the outcome of ignition depends on the temperature profile (Seitenzahl et al. 2009), this simulation also does not definitively reveal whether a SN Ia explodes. Consideration of the magnetic field evolution of the merger product of $M_1 + M_2 < M_{Ch}$ WD (Zhu et al. 2015) has shown that an exponential amplification of the field strength occurs. Zhu et al. speculated that the magnetic field provides a mechanism for angular momentum transfer and additional heating, facilitating carbon fusion.

It was pointed out earlier (Piersanti et al. 2003b), however, that, if a Keplerian disc forms out of the disrupted component and persists, as a result of the spin-up of rotation of the WD by accretion, instabilities associated with rotation, deformation of the WD, and angular momentum loss by a distorted configuration via gravitational waves, the accretion rate onto the WD that is initially $\sim 10^{-5}\ M_\odot\ yr^{-1}$ decreases to $4 \times 10^{-7}\ M_\odot\ yr^{-1}$, and close-to-centre ignition of carbon becomes possible. This self-regulated accretion mechanism is applicable for pairs with total mass (1.4–1.5) $M_\odot$ at the onset of carbon ignition; its time-scale is $\sim 10^6$ yr,

Kashyap et al. (2015) performed a post-merger evolution simulation for a (1.1+1.0) $M_\odot$ CO+CO WD system and found that a spiral-mode instability developed in the accretion disc on the dynamical time-scale and forced hot disc material to accrete onto the core of the remnant. This process drives a thermonuclear outburst, leading to a SN Ia without the need for artificial ignition. This mechanism works on a time-scale that is 2–3 orders of magnitude shorter than that of the magneto-rotational instability suggested by Ji et al. (2013). Thus, a self-ignited detonation may be possible in the post-merger stage at least for the most massive objects. Follow-up modelling of the light-curve and spectrum of the system (van Rossum et al. 2016) led to the suggestion that a better agreement with the observables of normal SNe Ia will require lower masses of components; however, whether a similar mechanism will be

effective for these systems remains an open question. Nevertheless, as noted by Kashyap et al. (2015), a wide range of He+CO WD mergers may ignite unstable He burning via the spiral-wave mechanism. An attractive feature of the above-described mechanism is that detonation occurs within ∼100 s of merger and the ejectum will not interact with any significant amount of the matter lost from the disc and produce additional radiation in the early light-curve, which may be misinterpreted in favour of the presence of a non-compact progenitor (Levanon, Soker & García-Berro 2015).

Note that in contrast to the simulations of SNe Ia by some authors, Dan et al. (2012), Dan et al. (2014), Moll et al. (2014), Sato et al. (2015) and Sato et al. (2016) took as initial models for exploration of the possibility of SN Ia the models obtained by computations of WD mergers, instead of taking an equilibrium hydrostatic model or a model obtained by the accretion of He onto CO WDs. It is assumed initially that WDs rotate synchronously (Fuller & Lai 2012; Burkart et al. 2013). In the case of non-synchronous rotation, disruption of the lower-mass WD occurs on a shorter time-scale (∼10 $P_{\rm orb}$) and is more 'violent' (Dan et al. 2011). In the case of asynchronous initial rotation, nuclear burning starts at higher densities, and it is more probable that SN Ia occur (e.g. Pakmor et al. 2012, 2013). As noted by Dan et al. (2014), it is likely that in the latter case detonation occurs in the centre of the merger product, while in the former case, at the core surface. As a result, there may be differences in the amount of unburned matter, ejectum velocity and ejectum asymmetry. However, the issue of initial conditions still remains controversial.

A special case is the still poorly explored mergers involving ONe WDs. If the disrupted dwarf is He-rich, one may expect He detonation followed by core collapse, if the remaining mass exceeds $M_{\rm Ch}$. Such a SN would be classified as a SN Ib (e.g. Kitaura, Janka & Hillebrandt 2006). Whether He detonation can in this case robustly trigger close-to-centre detonation remains an unsolved problem (Shen & Bildsten 2014). Marquardt et al. (2015) speculated that thermonuclear runaway in the core of ONe WDs *may* be triggered externally, and explored such a detonation. They concluded that observationally such explosions will be quite similar to the SNe Ia produced by detonations of CO WDs with a similar mass.

To summarize, a clear apprehension of the nature of progenitors of SNe Ia in the DD scenario and of the processes occurring during the merger of WDs and in the post-merger stage is currently lacking.

3 THE MODEL

For clarity, we reproduce in Fig. 1 a slightly modified $M_{\rm acc}$–$M_{\rm don}$ diagram for merging WDs (Dan et al. 2014), which we split into 13 subregions (zones) where pairs of WDs of different mass and chemical composition merge and different outcomes of merger are possible, including SNe Ia. We set the lower mass limit for possibly detonating He WDs at 0.37 $M_\odot$; above this limit, detonations in the stream and at the contact are possible (Dan et al. 2011, 2012), although, according to Holcomb et al. (2013), virialized He WDs even with $M_{\rm He} \geq 0.24$ $M_\odot$ may detonate. Despite the fact that the maximum mass of degenerate He cores of stars slightly decreases with stellar mass (Sweigart & Gross 1978), we use the 'canonical' value of 0.47 $M_\odot$ as the lower limit for the masses of CO WDs produced by asymptotic giant branch (AGB) stars. We also consider 'hybrid' WDs. As for He WDs, the lower boundary of the mass range of exploding hybrid WDs is set to 0.37 $M_\odot$.

Because we aim to evaluate the upper limit of the SNe Ia rate provided by the merging of WDs, we consider as SNe Ia all mergers of CO and He or hybrid WDs in which at least one detonation event is expected, although, as shown in the previous section, this issue is still open. It is unknown whether all such events will be identified with SNe Ia.

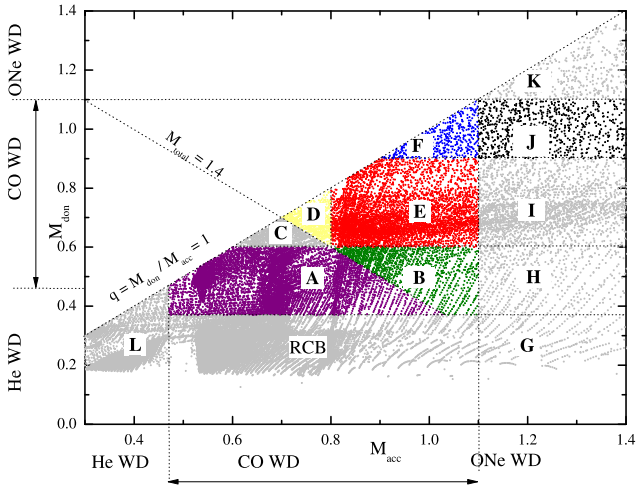

Figure 1. Breakdown of the $M_{\rm acc}$–$M_{\rm don}$ diagram into subregions. See the text for a detailed description. The density of dots in the particular regions of the diagram is proportional to the number of pairs of WDs that merge over 10 Gyr after an instantaneous star-formation burst for simulations with $Z = 0.02$, $\alpha_{\rm ce}\,\lambda = 2$, and tidal effects taken into account.

We expect the following events in the zones marked in Fig. 1.

A. Merger of a He or hybrid WD with a CO WD, resulting in He detonation in the envelope and possible subsequent detonation of carbon in the core.

B. Merger of a He or hybrid WD and a CO WD, resulting in the detonation of both WDs.

C. Merger of CO WDs with $M_1 + M_2 < M_{\rm Ch}$, with the formation of a massive single WD.

D. Merger of comparable-mass CO WDs, with an explosion in the post-merger process.

E. Merger of massive CO WDs, leading to SN Ia in the post-merger stage.

F. Merger of similar-mass CO WDs with an SN Ia explosion in the merger process.

G. Merger of a massive He WD or a hybrid WD with a ONe WD, with subsequent AIC.

H. Merger of an ONe WD with a hybrid WD, with subsequent AIC.

I. Merger of a CO WD and an ONe WD, with subsequent AIC of the ONe core.

J. Violent merger of an ONe WD with a CO WD, resulting in C detonation with subsequent detonation of the ONe WD (Marquardt et al. 2015). Dan et al. (2012) have shown that carbon-transferring systems do not detonate at contact.

K. Merger of ONe WDs. Thermonuclear explosion is possible, if the envelopes contain He. Such an event may be classified as a SN Ib rather than a weak SN Ia.

L. Merger of low-mass He or hybrid WDs, leading to the formation of He subdwarfs. No SN Ia are produced.

RCB. Merger of He and CO WDs in which the necessary conditions for He detonation are not met. Hypothetically, such mergers may lead to the formation of R CrB stars (Webbink 1984; Iben, Tutukov & Yungelson 1996); evolution of the latter is defined by competition of core growth owing to He shell burning and mass loss by the stellar wind. The growth of the core mass to $M_{\rm Ch}$ and explosion are not very likely, but, if they happen, the event would probably be observed as a peculiar SN Ib.

In assigning SN Ia status to the outcome of merger, we used, primarily, the numerical results and qualitative considerations presented in Dan et al. (2014, 2015), as well as data from the literature discussed in Section 2. Accordingly, we consider as SNe Ia results of mergers occurring in the zones **A**, **B**, **D**, **E**, **F** and **J**, although we recognize that all of them are still hypothetical. We note the following. If detonation of He in the pairs merging in the zones **A** and **B** does not initiate CO-core detonation, He explosions may be still identified with subluminous SNe Ia (Shen et al. 2010; Waldman et al. 2011). In zone **C**, mergers do not result in SNe Ia according to equation (1); furthermore, $M_{\rm a}$ should exceed about 0.8 $\rm M_{\odot}$. In zone **D**, undisrupted CO WDs accumulate $M_{\rm Ch}$ via self-regulating accretion in $\sim 10^6$ yr (Piersanti et al. 2003a). For mergers in zones **E** and **F**, the status of SN Ia is assigned according to the results of Sato et al. (2015) and of Moll et al. (2014) and Kashyap et al. (2015), respectively. Regarding possible explosions of ONe WDs, Marquardt et al. (2015) have shown that detonations of these objects are possible, given that there is an external trigger. Appropriate computations are absent, but it is clear that the 'trigger' dwarf has to be massive or such events may not happen at all. Thus, our limiting $M_{\rm d} = 0.9$ $\rm M_{\odot}$ may be too optimistic. Note, however, that the contribution of zone **J** to the rate of SNe Ia in the case $\alpha_{\rm ce}\,\lambda = 2$, which we consider as giving the best agreement with observations, does not exceed 10 per cent (see Section 4).

3.1 Population synthesis

In order to model the population of merging WDs, we applied the code BSE (Hurley, Pols & Tout 2000; Hurley, Tout & Pols 2002; Kiel et al. 2008). The advantage of BSE is that it is based on a homogeneous system of evolutionary tracks for single stars with metallicity from Z = 0.0001 to 0.02 (Pols et al. 1998), which was used to construct analytical approximations describing stellar evolution. The shortcoming of BSE is that the evolution of binaries is treated on the basis of assumptions originating from the work of other authors or of (educated) guesses for never-calculated evolutionary transitions.

Our results are based on the modelling of 10^7 initial systems, and for each set of initial parameters represent one realization of the model. Hence, they are subject to Poisson noise.

Taking into account recent suggestions on the dependence of the binarity rate on the mass of stars, we approximated this rate as (van Haaften et al. 2013)

$$f_{\rm b} = 0.50 + 0.25\log(M_1/\,\rm M_{\odot}). \qquad (2)$$

Common envelopes. The problem of common envelopes (CEs) is the most acute one in the theory of the evolution of close binaries; see Ivanova et al. (2013) for a recent detailed discussion. In the context of the problem we address in the present study, CEs form when the accretor is not able to swallow all the matter supplied by the donor, or the system is subject to the Darwin instability. There is no unanimous opinion on the form of the equation describing the evolution of stars in the CE. We apply an equation suggested by Tout et al. (1997), included in BSE as an option, because in our opinion it better accounts for the expenditure of energy on the expulsion of the CE than the 'standard' (Webbink 1984; de Kool 1990) equation, if both components have clear-cut cores and envelopes. However, test runs with the 'standard' equation show that the difference in the rates of SNe Ia does not exceed 10 per cent. The basic problem of both formulations of the CE equation is that its solution for the ratio of the initial and final separations of the components, upon which it is decided whether the components merged, depends on the product of two parameters – $\alpha_{\rm ce}\,\lambda$. The 'common envelope efficiency' $\alpha_{\rm ce}$ describes the efficiency with which the spiralling-in cores of components transfer orbital energy to the envelope and disperse the latter; it is expressed in fractions of the orbital energy of the system, parameter λ characterizes the binding energy of the donor envelope.

A problem related to the outcome of the CE was noted by Kashi & Soker (2011): while CE equation(s) may formally imply that the system remains detached at the end of the CE stage, in fact some matter of the envelope may not reach escape velocity and instead remain bound to the system forming a circumbinary disc. Angular momentum loss owing to interaction with the disc may result in a further reduction of the binary separation and the merger of components. This may influence, among other populations, SNe Ia, but this problem remains unsolved. On the other hand, the influence of this phenomenon is compensated by uncertainty in the treatment of CEs in general.

Both parameters describing the CE are still highly uncertain. For $\alpha_{\rm ce}$, the most important issue is whether there are other sources than orbital energy for the expulsion of CEs; that is, whether $\alpha_{\rm ce} > 1$ is possible. In fact, $\alpha_{\rm ce}$ is a specific parameter of any CE. The use of it is forced, because for a given system with components at different evolutionary stages, particular combination of M_1, M_2, a, the outcome of the CE can be found only by 3D hydrodynamical calculations, which still have insufficient resolution or do not account for all physical processes occurring in CEs on different time-scales (Ohlmann et al. 2016). It is evident that λ should continuously vary in the course of stellar evolution; the position of the core–envelope boundary remains uncertain – the value of λ may be uncertain by a factor of 10 depending on the definition of the core–envelope boundary (Tauris & Dewi 2001). Regarding 'observational' estimates, the existence of severe selection effects should be noted, which may restrict the observed population to fractions of a per cent of the intrinsic one, resulting in poor statistics (see e.g. Camacho et al. 2014).

Nevertheless, we consider it justified to use as a constant parameter the value(s) of $\alpha_{\rm ce}$ found for sufficiently representative samples of close binaries that evolved through the CE stage or were derived from the study of particular binaries. However, it appears, for instance, that for low-mass systems – post-CE binaries (PCEB) with $M_2 \lesssim 0.8$ $\rm M_{\odot}$ from SDSS – the estimates of $\alpha_{\rm ce}$ range (within error bars) between 0.02 and 10 (Zorotovic et al. 2010). Within this range, for the systems with AGB progenitors, $\alpha_{\rm ce}$ values cluster below 0.2, while for those with the first giant branch (FGB) progenitors, almost all $\alpha_{\rm ce}$ values are $\gtrsim$0.2. Thus, the quite common claim that $\alpha_{\rm ce} \approx 0.2 - 0.3$ seems to be not well justified. The population of well-studied binary WDs, after accounting for observational selection, is well reproduced with $\alpha_{\rm ce}\,\lambda = 2$ (Nelemans et al. 2001a; Toonen, Nelemans & Portegies Zwart 2012). Therefore, we performed simulations for $\alpha_{\rm ce}\,\lambda$ in the range from 0.25 to 2, but consider the version with $\alpha_{\rm ce}\,\lambda = 2$ as the main version; see Section 4. In a similar way, in their studies of SNe Ia, Mennekens et al. (2010) parametrized CEs by $\alpha_{\rm ce}\,\lambda = 1$, while Toonen et al. (2012, 2014) used $\alpha_{\rm ce}\,\lambda = 2$.

Stability of mass exchange. An under-researched topic in binary star evolution is the stability of mass loss by stars with deep convective envelopes and He stars. For H-rich stars, we kept the stability criteria accepted in the BSE code. For He stars – the remnants of components of binaries with mass $\gtrsim$(2.0 − 2.5) $\rm M_{\odot}$, which experienced RLOF in the H-shell-burning stage (Case B of mass exchange), the stability criteria were modified. Paczyński (1971) and Iben & Tutukov (1985) showed that He stars with masses below (0.8–0.9) $\rm M_{\odot}$ do not expand after He exhaustion in their cores

and evolve straight into hybrid WDs. More massive He stars expand in the He-shell-burning stage; the extent of the expansion depends on the mass of the star, and RLOF may restart if the components are close enough.

Based on trial computations of semidetached binaries with He donors (D. Kolesnikov et al., in preparation) we consider mass loss unstable if the stellar radius becomes ≥ 5 $R_\odot$ and $q \geq 0.78$. If R_{He} remains below 5 $R_\odot$, the critical $q = 3.5$.

Angular momentum loss via gravitational wave radiation may bring low-mass He stars into contact with WDs prior to He exhaustion in their cores. In the systems where conditions for stable mass exchange are fulfilled, initially $\dot{M} \sim 10^{-8}\,M_\odot\,yr^{-1}$ (Savonije, de Kool & van den Heuvel 1986; Iben & Tutukov 1991; Yungelson 2008). At these values of $\dot{M}$, surface detonation of He is possible (Taam 1980; Nomoto 1982). We exclude such systems from further consideration, because they are not of interest in the present study. Such binaries are suggested to be progenitors of double-detonation SN Ia, but the real efficiency of this scenario is under debate (Piersanti, Tornambé & Yungelson 2014; Piersanti, Yungelson & Tornambé 2015; Brooks et al. 2015).

For WDs, the stability of mass exchange depends on the mass ratio of components and the efficiency of spin/orbit coupling (Nelemans et al. 2001b; Marsh et al. 2004). In addition, it is possible that tidal interaction allows stable mass transfer, but the rate of the latter is super-Eddington and a CE may form. We considered mass transfer between WDs to be stable, irrespective of the efficiency of spin/orbit coupling, if its rate remains sub-Eddington and M_{don} (in solar units) satisfies the following approximation based on fig. 1 of Dan et al. (2011):

$$M_d \leq \begin{cases} 0.2286\,M_{acc}, & \text{if } M_{acc} \leq 0.875; \\ 0.133\,M_{acc} + 0.0833, & \text{if } 0.875 < M_{acc} \leq 1.1; \\ -0.033\,M_{acc} + 0.2667, & \text{if } 1.1 < M_{acc} \leq 1.44. \end{cases} \quad (3)$$

Tidal effects. Tidal effects are significant predominantly for giant stars. The main evolutionary consequence of tides is an earlier RLOF if the tides are taken into account. For instance, RLOF in the RG stage instead of the AGB stage may occur and a He or hybrid WD form instead of a CO WD. On the other hand, for later RLOF, the formation of a CE and merger of components there is more probable. There is no consensus on the account of tides in binary population synthesis (BPS); see the comparison of assumptions in table 1 of Toonen et al. (2012). For instance, they were not taken into account in the latest simulations of Claeys et al. (2014). We used the algorithm for the account of circularization of the orbits and synchronization of rotation as it is incorporated in BSE, that is, according to Zahn (1975) for stars with radiative envelopes and according to Hut (1981) for stars with convective envelopes.

We implemented modifications in the code to the algorithm for the computation of the mass-transfer rate that make it more stable (Claeys et al. 2014, equation 11).

Star-formation rate. For the estimate of the SNe Ia rate in the Galaxy, we accepted that the star-formation rate (SFR) in the bulge and thin Galactic disc can be described by a function combining exponentially declining and slow constant components (Yu & Jeffery 2010):

$$SFR(t) = 11\exp(-(t - t_0)/\tau) + 0.12(t - t_0)\,M_\odot\,yr^{-1} \text{ for } t > t_0. \quad (4)$$

Here, time t is in Gyr, τ=9 Gyr, t_0=4 Gyr, and the Galactic age is 14 Gyr. We neglect halo and thick Galactic disc stars with a total mass of only several per cent of the mass of the bulge and the thin disc. In the bulge and thin disc, $SFR(t) = 0$ at $t \leq t_0$. The current Galactic SFR is 4.82 $M_\odot\,yr^{-1}$, well within the range of modern estimates, namely from ∼1 to ∼10 $M_\odot\,yr^{-1}$ (Gilmore 2001). The total mass of the bulge and the disc is then 7.2×10^{10} $M_\odot$, close to the estimate of Klypin, Zhao & Somerville (2002) of 7.0×10^{10} $M_\odot$.

We neglect stellar winds of He stars in the calculations, because the extrapolation of the rates of Wolf–Rayet stars or Reimers-type winds assumed in BSE is not justified and, even then, it is hardly evolutionary meaningful because of the extremely short lifetimes of He stars.

4 RESULTS

4.1 Scenarios for the formation of merging white dwarfs

Population synthesis calculations generate hundreds of evolutionary scenarios. However, the dominant fraction of merging WDs of interest usually form through only a few channels, differing mainly by the stage at which the more massive component initially overflows its Roche lobe. Despite the fact that these scenarios have been analysed many times, starting from semi-analytical studies by Tutukov & Yungelson (1981), Iben & Tutukov (1984) and Webbink (1984), and, most recently, by for example Ruiter, Belczynski & Fryer (2009), Mennekens et al. (2010), Toonen et al. (2014) and Claeys et al. (2014), they still deserve attention.

The fraction of stars evolving via certain channels depends mainly on the accepted criteria of the stability of mass loss, the treatment of CE stage(s), the mass and momentum loss from the system, the treatment of accretion onto compact stars, and criteria according to which the stars are considered as 'merged'. For instance, compare the simulations of Mennekens et al. (2010) and Toonen et al. (2012), which differ in the assumed radii of stellar remnants and $\alpha_{ce}\,\lambda$ values: 1 in Mennekens et al. (2010) and 2 in Toonen et al. (2014). In the first study, 80 per cent of CO WDs and CO cores of donors merge in the CE, while in the second one only 45 per cent do.

Eight main scenarios, which in our simulations result in the formation of not less than about 90 per cent of all merging pairs of WDs, considered as possible precursors of SN Ia are shown in Table 1. The table corresponds to Z = 0.02, $\alpha_{ce}\,\lambda = 2$, and tides are taken into account. We apply with slight modification the notation accepted in BSE and widely used in the literature: MS, main-sequence star; HG, Hertzsprung gap star; GB, first giant-branch star; CHeB, a star with central He burning; EAGB and TPAGB, early and thermally pulsating AGB stars, respectively; HeMS, He-burning remnant of a star; HeWD, COWD, ONeWD, helium, carbon–oxygen and oxygen–neon white dwarfs, respectively. We consider He-shell-burning 'helium Hertzsprung-gap' (HeHG in BSE) stars and 'helium giants' (HeG in BSE) as similar objects with CO cores and He-burning shells, because they differ only in the extent of expansion of He envelopes. They are identified in Table 1 and in the text as 'COHe'. For the pairs of WDs produced by a certain scenario, we indicate at pre-merger stage the most common combination of components: for instance, scenario 1 is marked as forming a CO WD+CO WD pair, while in fact about 25 per cent of pairs contain ONe components, owing to a 'change of the roles' during RLOF when initially less-massive secondaries accumulate large mass; we do not consider pairs with ONe WDs for computation of SNe Ia rates etc. In Appendix A, in Figs A1–A8, we show for these scenarios the positions of the initial systems in $M_{1,i} - M_{2,i}$, $M_{1,i} - a_i$ and pre-merger M_{acc}–M_{don} diagrams. The plots are for the $\alpha_{ce}\,\lambda = 2$ case, in which the mergers of WD occur most efficiently (see below).

Table 1. Main evolutionary tracks leading to the formation of merging white dwarfs and possible SN Ia. First row: number of the sequence; second row: evolutionary stage preceding the first common envelope episode. A brace by the component identifier means that this star overflows its Roche lobe. The absence of a brace means that the system is detached. Stages with similar outcomes are joined by horizontal braces. 'CE1' and 'CE2' denote the first and the second common envelope episodes, respectively. For the rest of the notation, see the text. Down-arrow symbols indicate that in a particular scenario certain evolutionary stages are absent.

	1	2	3	4
	COWD+HG	COWD+GB	COWD+EAGB	HeMS+GB
1	MS+MS	MS+MS	MS+MS	MS+MS
2	HG+MS	↙ ↘	HG+MS	HG+MS
3	{HG+MS	{HG+MS HG+MS	{HG+MS	{HG+MS
4		{GB+MS {GB+MS	{GB+MS	{GB+MS
5	{GB+MS		↙ ↘	⇓
6	HeMS+MS	HeMS+MS	HeMS+MS {GB+MS	HeMS+MS
7	COHe+MS	↙ ↘	↓ ↘ ↙	HeMS+HG
8	{COHe+MS	{COHe+MS COHe+MS	{COHe+MS HeMS+MS ⇓	↙ ↘
9		{COHe+MS	COHe+MS ⇓	{COHe+GB HeMS+GB
10				HeMS+GB}
11	COHe+MS			
12	COWD+MS	COWD+MS	COWD+MS	**CE1**
13	COWD+HG	COWD+HG	COWD+HG	
14	COWD+HG}	COWD+GB	COWD+GB	HeMS+HeMS
15		COWD+GB}	COWD+CHeB	
16			COWD+EAGB	COHe+HeMS
17			COWD+EAGB}	
18	**CE**	**CE1**	**CE1**	COWD+HeMS
19		↙ ↘		
20	COWD+HeMS	COWD+HeWD COWD+HeMS		
21	COWD+COHe	COWD+COHe	COWD+COHe	COWD+COHe
22		↙ ↘	↙ ↘	COWD+COHe}
23	COWD+ COHe}	⇓ COWD+COHe COWD+COHe}	COWD+COHe} COWD+COHe	↙ ↘
24		**CE2**	**CE2**	⇓ **CE2**
25	⇓	⇓		
26		⇓	⇓	
27	COWD+COWD	COWD+HeWD COWD+COWD	COWD+COWD	COWD+COWD COWD+ONeWD
28	{COWD+COWD	COWD+HeWD} COWD+COWD}	COWD+COWD}	{COWD+COWD COWD+ONeWD}
29				
30		**Merger**		

	5	6	7	8
	EAGB+ CHeB	TPAGB+ CHeB	EAGB+MS	TPAGB+MS
1		MS+MS	MS+MS	MS+MS
2		HG+MS	HG+MS	HG+MS
3			GB+MS	GB+MS
4			CHeB+MS	CHeB+MS
5	↙	↘	EAGB+MS	EAGB+MS
6	GB+MS	HG+HG		
7			{EAGB+MS	TPAGB+MS
8				{TPAGB+MS
9			**CE1**	**CE1**
10		GB+HG	COHe+MS	
11		GB+GB	↙ ↘	⇓
12			{COHe+MS	
13			⇓	⇓
14		CHeB+GB	COHe+MS	
15		CHeB+CHeB	COWD+MS	COWD+MS
16		↙ ↘	COWD+HG ⇓	COWD+HG
17	EAGB+CHeB	EAGB+CHeB		↙ ↓ ↘
18	{EAGB+CHeB	TPAGB+CHeB		COWD+HG}
19			COWD+HG}	
20			COWD+GB}	COWD+GB} COWD+GB
21		{TPAGB+CHeB		COWD+CHeB
22				⇓ ⇓ COWD+EAGB
23				COWD+EAGB}
24				
25	**CE1**		**CE2**	**CE2**
26				↙ ↘
27		COWD+HeMS	COWD+HeMS	COWD+HeMS
28		COWD+COHe	COWD+COHe	
29			COWD+COHe}	COWD+COHe} COWD+COHe
30				
31			COWD+COWD	
32			COWD+COWD}	
33				
34			**Merger**	

In scenarios 1 to 4, the first CO WD forms via stable RLOF, starting in the Hertzsprung gap or in the first RG branch (case B of mass exchange). This results in the formation of a He star. As noted, the latter may evolve straight into a CO WD, if their mass is $\lesssim(0.8 - 0.9)$ $M_\odot$ or refill the Roche lobe and lose some mass (in small-separation systems) for a short time when the star expands on the thermal time-scale in the He-shell burning stage. Because the first RLOF is stable, the secondaries typically accumulate mass greater than ≈ 2 $M_\odot$, and after mass loss become He stars. He WDs appear only in the side branch of scenario 2 after the CE, if $M_2 \lesssim 2.25$ $M_\odot$. Most merging CO WD+He WD pairs are actually formed by several scenarios that are not among the most prolific ones.[4]

Scenario 1 involves stars more massive than $\simeq 4$ $M_\odot$. Because the masses of the components are relatively comparable (Fig. A1), both resulting WDs are quite massive and feed predominantly zones **E**, **F** and **J**.

Systems with $3 \lesssim M_1/M_\odot \lesssim 8$ evolve via scenario 2, but on average the secondaries are less massive than in scenario 1. This scenario is similar to scenario 1, but because of the larger span of the initial masses of components it contributes merging pairs of CO WDs to virtually all zones of the $M_{\rm acc}$–$M_{\rm don}$ plane (Fig. A2). Because the secondaries in some of the initial systems evolving via scenario 2 have initial masses as small as almost 1 $M_\odot$, certain fraction of former secondaries after mass loss in the CE becomes He WDs. However, scenario 2 is not the main channel of He WD formation; most of them form, as mentioned above, via non-common routes. In total, in scenario 2 the fraction of merging He and CO WD pairs feeding zone **A** in Fig. 1 among all merging pairs is 7 per cent for $\alpha_{\rm ce}\,\lambda = 0.25$, 8 per cent for $\alpha_{\rm ce}\,\lambda = 0.5$, 0.3 per cent for $\alpha_{\rm ce}\,\lambda = 1.0$ and 4.5 per cent for $\alpha_{\rm ce}\,\lambda = 2.0$. Most CO and He WDs merge in zone **L**, where they produce hot subdwarfs, or in zone **R CrB**; see Fig. 1.

Binaries with $2.5 \lesssim M_1/M_\odot \lesssim 8$ $M_\odot$ and less massive secondaries than in the previous scenarios – $M_2 \lesssim 4$ $M_\odot$ – evolve via scenario 3. After the first stable mass exchange, these systems become so wide that former initial secondaries overflow the Roche lobe only in the early AGB stage. Their C/O cores are small, however, and after mass loss in the CE the stars still have relatively massive He envelopes and their evolution is similar to the evolution of He stars. This scenario contributes to the regions of the $M_{\rm acc}$–$M_{\rm don}$ diagram where a single detonation of He (**A**) or a merger of a CO WD with $M_1 + M_2 \geq M_{\rm Ch}$ (**E, F**) is possible (Fig. A3).

Scenario 4 is followed by systems with $2 \lesssim M_1/M_\odot \lesssim 7$, with initial separations of the components on average smaller than in scenario 3 (Fig. A4). For this reason, prior to the CE, secondaries are still in the RGB- stage of evolution, and after mass loss produce He stars. The least massive of He stars evolve straight into hybrid CO WDs, while more massive ones expand and the system passes through a second CE (Table 1). If $\alpha_{\rm ce}\,\lambda \leq 0.5$, scenario 4 produces also some ONe WD+CO WD pairs and makes a small contribution to zone **J** (Table 2).

In scenarios 5–8, in contrast to scenarios 1–4, the first RLOF in the system is accompanied by a CE. These systems are wide, the primaries overflow their Roche lobes in the EAGB and TPAGB stages of evolution (case C of mass exchange), and mass loss is dynamically unstable. Scenarios 5 and 6 (Figs A5, A6) are quite similar. Through these scenarios evolve systems that have components with similar masses. At the time of the first RLOF, the companions to mass-losing stars are in the core He-burning stage (Table 1), and the compact cores of both stars appear to be immersed in a 'double common envelope'. The result of the CE stage is the formation of a CO WD+He MS binary. Merging pairs contain either a CO WD and a hybrid WD or two CO WDs. The outcome of the merger may be single detonation (zone **A**), the formation of a massive CO WD (zone **C**), or the merger of (super)-$M_{\rm Ch}$ CO WDs (zones **D** and **E**).

Scenarios 7 and 8 (Figs A7, A8) relate to the evolution of the widest close binaries with secondaries within quite a large range from 2.5 $M_\odot$ to almost 5 $M_\odot$. The primaries in these stars overflow their Roche lobes in the EAGB or TPAGB stage, while their companions remain MS stars. A CE stage follows. In scenario 7, the donor with a small He core first becomes a COHe star and later, a CO WD. In scenario 7, the separation of components is such that former secondaries overflow their critical lobes in the HG or GB stage and turn into He stars. After exhaustion of He in the cores they evolve into CO WDs. Scenario 7 feeds the 'massive' part of the sub-$M_{\rm Ch}$ zone **B**, where both WDs may explode at contact, and zone **E**, where (super)-$M_{\rm Ch}$ CO WDs merge. In scenario 8, with the wider initial separation of the components, a CO WD is formed straight after the first CE, while the former secondary may, depending on the initial mass and separation, overflow the critical lobe in the HG, GB or EAGB stage. In all cases, a CE forms, and He stars are formed, which later evolve into CO WDs. As for scenario 7, scenario 8 feeds the massive-WD part of zone **A** and zone **E**.

It is worthwhile to note that, while the precursors of most observed binary WDs apparently form via two stages of the CE (Toonen et al. 2012), most progenitor binaries of merging pairs of WDs in our simulations have a stable first mass-exchange episode and then an unstable (with a CE) second one, as also found by Mennekens et al. (2010) and Ruiter et al. (2013). In the simulations of Toonen et al. (2012), the fraction of systems which have only one CE stage is close to 50 per cent.

Above, we presented scenarios dominating in the $\alpha_{\rm ce}\,\lambda = 2$ case. Some scenarios are not realized for all $\alpha_{\rm ce}\,\lambda$. Furthermore, their relative input varies with $\alpha_{\rm ce}\,\lambda$. In Table 2 we compare the fractions of systems evolving via the scenarios listed in Table 1, depending on $\alpha_{\rm ce}\,\lambda$ and their input to the particular regions of the $M_{\rm acc}$–$M_{\rm don}$ diagram. Because of the uncertainty in the value of $\alpha_{\rm ce}\,\lambda$ we studied the demography of the $M_{\rm acc}$–$M_{\rm don}$ diagram for $\alpha_{\rm ce}\,\lambda = 0.25$, 0.5, 1.0 and 2.0.

For $\alpha_{\rm ce}\,\lambda = 0.25$, essentially only scenario 3 can result in the formation of a merging pair of WDs and a SN Ia. Because $\alpha_{\rm ce}\,\lambda$ is low, this may be understood as a result of the merger of components in CE1 or CE2 in other scenarios. Two branches of evolution can be distinguished, leading, predominantly, to the filling of regions **A** and **E** of the $M_{\rm acc}$–$M_{\rm don}$ plane. In the first case, a CO WD merges with a hybrid or a He WD, while in the second one, two CO WDs with $M_1 + M_2 \geq M_{\rm Ch}$ merge. The contribution to the two zones is comparable. For $\alpha_{\rm ce}\,\lambda = 0.25$ no systems evolve via scenario 1; that is, mergers of CO and ONe WDs do not occur and the 'triggering' of explosions of ONe WDs simulating SN Ia (Marquardt et al. 2015) is infeasible. For other values of $\alpha_{\rm ce}\,\lambda$, the significance of this scenario is vanishingly small.

Scenario 3 dominates for $\alpha_{\rm ce}\,\lambda = 0.5$ and 1 and feeds predominantly zones **A** and **E** of the $M_{\rm acc}$–$M_{\rm don}$ diagram. With an increase in $\alpha_{\rm ce}\,\lambda$, the contribution of this scenario to zone **A** first increases, because a larger fraction of low-mass CO WDs avoids merger.

[4] In the original version of BSE, as He WD are annotated also low-mass remnants of core-helium-burning stars which experienced stable RLOF and have mass lower than conventional mass-limit for He-burning of 0.32 $M_\odot$. In fact, in such stars nuclear burning is frozen almost immediately after Roche lobe overflow, and their interiors may vary from almost pure He to a C/O mixture, depending on the degree of exhaustion of He in the centre at the instant of RLOF. Their entropy is lower than that of He WDs – former degenerate cores of red giants (Yungelson 2008). These stars may be donors in systems experiencing single He detonation or double-detonation.

Table 2. Relative numbers of mergers, possible precursors of SNe Ia, occurring in particular zones of the M_{acc}–M_{don} diagram over 10 Gyr, for various values of $\alpha_{ce}\,\lambda$. Column (1), $\alpha_{ce}\,\lambda$; Column (2), number of scenario according to Table 1; Column (3), evolutionary stage of the system preceding the first CE. Columns (4) to (9) with headers A to J indicate the relative numbers (in per cent) of WD pairs formed via scenarios listed in column (2) and merging in particular zones of the M_{acc}–M_{don} diagram (Fig. 1) over 10 Gyr. Column (10), relative input of a particular scenario into the total rate of WD+WD mergers for a given $\alpha_{ce}\,\lambda$. Column (11), ratio of the number of mergers of possible precursors of SN Ia and total number of merging WD pairs for every channel and $\alpha_{ce}\,\lambda$ value. The absence of data on some scenarios for certain $\alpha_{ce}\,\lambda$ means that for this $\alpha_{ce}\,\lambda$ the code does not generate such a scenario at all.

	Scen.	Stage	Zone of M_{acc}–M_{don} diagram						SNIa	$N_{SNIa}/$
$\alpha_{ce}\,\lambda$		before CE1	A	B	D	E	F	J		N_{WD2}
(1)	(2)	(3)	(4)	(5)	(6)	(7)	(8)	(9)	(10)	(11)
0.25	2	COWD+GB	2.1	–	–	–	–	0.2	2.3	5.60E-03
0.25	3	COWD+EAGB	31.8	12.3	1.3	39.4	1.3	8.1	94.1	2.30E-01
0.25	4	HeMS+GB	–	–	–	–	–	0.6	0.6	1.40E-03
0.25	5	EAGB+CHeB	–	–	–	–	–	0.1	0.1	1.60E-04
0.25		Sum	33.8	12.3	1.3	39.4	1.3	8.9	97	2.40E-01
0.5	2	COWD+GB	1.4	0.2	–	1.4	–	2.8	5.8	9.20E-03
0.5	3	COWD+EAGB	50.3	2.9	5.4	24.3	0.7	2.2	85.7	1.30E-01
0.5	4	HeMS+GB	–	–	–	0.5	0.2	0.9	1.6	2.60E-03
0.5	5	EAGB+CHeB	0.8	–	–	–	–	0.2	1	1.60E-03
0.5	6	TPAGB+CHeB	0.2	–	–	–	–	0.02	0.3	4.20E-04
0.5		Sum	52.7	3.1	5.4	26.2	0.9	6.3	94.5	1.50E-01
1	1	COWD+HG	–	–	–	–	–	0.2	0.2	2.10E-04
1	2	COWD+GB	5.7	1.3	2.4	10.2	0.1	3.2	23	2.50E-02
1	3	COWD+EAGB	23.4	0.4	2.9	6.8	0.6	2	36.1	4.00E-02
1	4	HeMS+GB	5.1	1.1	3	14.2	0.1	–	23.4	2.60E-02
1	5	EAGB+CHeB	4.5	–	0.01	0.04	0.04	0.3	4.8	5.40E-03
1	6	TPAGB+CHeB	2.4	0.1	0.1	1.4	–	0.03	4	4.40E-03
1		Sum	41	2.9	8.5	32.6	0.8	5.7	91.5	1.00E-01
2	1	COWD+HG	–	–	0.2	0.5	0.4	1.1	2.1	5.00E-03
2	2	COWD+GB	9.2	0.5	1.7	5.4	1.2	1.7	19.7	4.60E-02
2	3	COWD+EAGB	2.9	–	0.6	1.3	0.2	0.5	5.5	1.30E-02
2	4	HeMS+GB	16.6	0.3	4.8	7.1	0.004	–	28.8	6.80E-02
2	5	EAGB+CHeB	5.8	–	0.5	0.5	0.02	0.1	7	1.60E-02
2	6	TPAGB+CHeB	2.8	0.04	0.2	0.8	–	0.02	3.9	9.20E-03
2	7	EAGB+MS	2.7	2.2	–	5	–	–	9.9	2.30E-02
2	8	TPAGB+MS	5.6	3.3	0.04	2.1	–	–	10.9	2.60E-02
2		Sum	45.6	6.3	7.9	22.9	1.8	3.3	87.8	2.10E-01

However, with a further increase of $\alpha_{ce}\,\lambda$ over 1, the separation of the components after the second CE episode remains so large that binaries never merge.

For $\alpha_{ce}\,\lambda = 1$, scenarios 2, 4 and 5 become significant. In general, as expected, with an increase of $\alpha_{ce}\,\lambda$the contribution of systems in which the RLOF occurs at later phases, i.e. wider at the zero-age main-sequence, increases.

For $\alpha_{ce}\,\lambda = 2$, scenarios 2 and 4 become dominant, and scenarios 5 and 8 provide a significant contribution to zones **A** and **E**. It is important that in all scenarios at least one of the merging WDs is a hybrid one and probably retains some He in the envelope up to the beginning of merger, and, in principle, may detonate. Formation of hybrid WD occurs because AGB evolution is typically aborted in quite an early stage, when the CO core is still not well developed, and the post-RLOF star continues its evolution as a star with a thick He envelope (COHe in our notation). The similarity between the outcome of cases B and early C of mass exchange was noticed by Iben (1986), but with a caveat that in the case of B the stellar remnants are less massive. If RLOF occurred in the TPAGB stage, the mass of the nascent WD is also higher than for RLOF in the EAGB case, because of the dredge-up event, which occurred in the course of evolution between two stages.

The trends observed in Table 2 are a relatively even (within a factor of 1.5) fractional population of regions **A** and **E** of the M_{acc}–M_{don} diagram, irrespective of the value of $\alpha_{ce}\,\lambda$ and the systematic decrease of the populations of regions **F** and **J**, associated with the most massive WDs, with an increase of $\alpha_{ce}\,\lambda$. Most mergers of WDs occur in zones **A** and **E** (Table 2); that is, as mergers of relatively massive He or hybrid WDs and CO WDs or pairs of CO WDs.

Table 2 clearly shows the influence of the combined parameter $\alpha_{ce}\,\lambda$ on the merger rate of WDs. In scenarios 1–4, most systems after the first, stable RLOF become so wide that, if the expulsion of the matter from the system in the CE is efficient (α_{ce} is low), the merger of the components is avoided and they form pairs of WDs that are close enough to merge in Hubble time. With an increase of α_{ce}, the fraction of merging pairs of WDs decreases. Fig. A3, as an example, illustrates the variation of the initial parameters of systems contributing to scenario 3 for two extreme cases of $\alpha_{ce}\,\lambda$ and the influence of this parameter on the masses and types of merging WDs.

We do not present results for the runs with $\alpha_{ce}\,\lambda > 2$ because such high values of $\alpha_{ce}\,\lambda$ currently seem unrealistic.

4.2 Delay-time distribution

The fundamental characteristic of SNe Ia is the DTD; that is, the distribution over time-intervals between the formation of a close binary and SN Ia explosion, because every scenario of SN Ia has a typical time-scale (Tutukov & Yungelson 1994; Ruiz-Lapuente, Burkert & Canal 1995; Jorgensen et al. 1997; Yungelson & Livio 2000). The empirical DTD is, as a rule, derived from the rate of SNe Ia in samples of galaxies at large redshifts ($z \sim 1$), but may

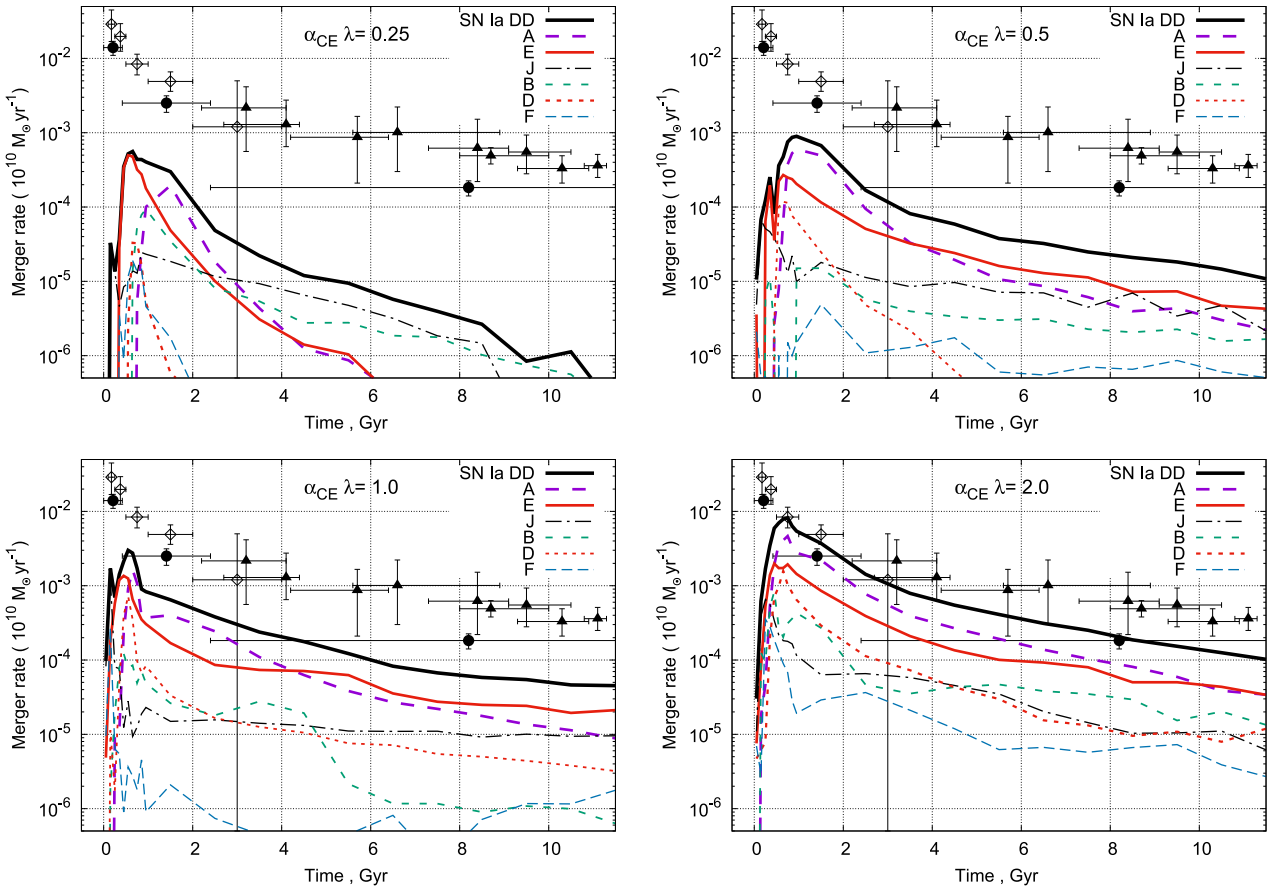

Figure 2. Delay-time distribution (DTD) for the model WD+WD mergers potentially producing SNe Ia. Different line styles represent mergers occurring in different zones of the $M_{\rm acc}$–$M_{\rm don}$ diagram, annotated as in Fig. 1. The thick solid line (SN Ia) represents the sum of the models. The models correspond to a metal abundance Z = 0.02. Symbols with error bars: 'observational' DTD from the Subaru/*XMM* Survey (Totani et al. 2008), diamonds; galaxy clusters (Maoz, Sharon & Gal-Yam 2010), triangles; a sample of field galaxies from the SLOAN II Survey (Maoz, Mannucci & Brandt 2012), heavy dots.

also be derived for individual galaxies; see Maoz et al. (2014). Theoretically, it is a model of the dependence of the rate of SNe Ia with different precursors on the time elapsed from an instantaneous burst of star formation that formed a unit of stellar mass. It is evident that hypothetical SNe Ia associated with short-lived objects, for example He stars, should have short delays ($\lesssim$1 Gyr). If, on the other hand, a particular scenario is associated with potentially long-lived objects such as a double-degenerate, delays for them may in principle overlap with the entire lifetime of a galaxy, because most massive WDs start to merge in several tens of millions of years after a star-formation burst, and the upper limit is the Hubble time. Both experimental and theoretical estimates of the DTD are overburdened by numerous uncertainties. For empirical estimates, uncertainty may reach an order of magnitude, depending on the sample of SNe Ia under study and possible systematic errors; see Maoz et al. (2014) for a detailed discussion and Fig. 2. The scatter in the theoretical estimates results mainly from the difference in the treatment of evolutionary transformations of binaries in different BPS codes (Toonen et al. 2014).

Fig. 2 shows the model DTD for the mergers of WDs potentially leading to SNe Ia and empirical data for elliptical galaxies from the Subaru/*XMM–Newton* Deep Survey (Totani et al. 2008), galaxy clusters (Maoz et al. 2010), and a sample of galaxies from the SLOAN II Survey (Maoz et al. 2012). Clearly, none of the models fit the observations at very early epochs ($\lesssim$500 Myr). Only models for $\alpha_{\rm ce}\,\lambda = 2$ fit points at $\approx$1 and 8 Gyr of the DTD derived for the

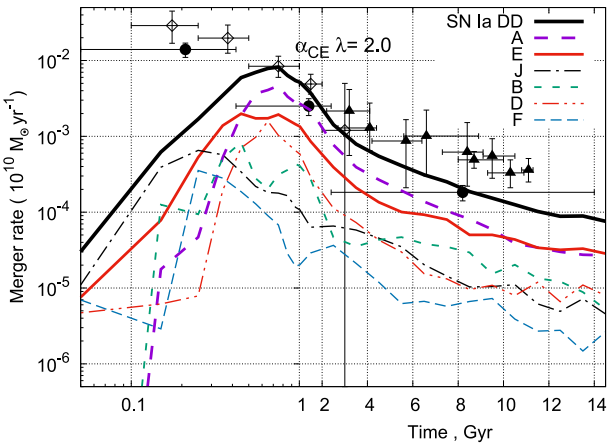

Figure 3. Delay-time distribution (DTD) for the model WD+WD mergers potentially producing SNe Ia in the case of $\alpha_{\rm ce}\,\lambda = 2$, similar to in the lower right panel of Fig. 2, but showing the DTD for the first 0.05–2 Gyr on a log-scale.

SLOAN II Survey, which has very large time-bins and error bars. If we consider the DTD for galaxy clusters, at $\approx$(7–10) Gyr, the difference approaches a factor close to 3–4. The main fraction of mergers occurs in the zones **A** and **E** of the $M_{\rm acc}$–$M_{\rm don}$ diagram. For illustration, at the request of the referee, in Fig. 3 we replot the

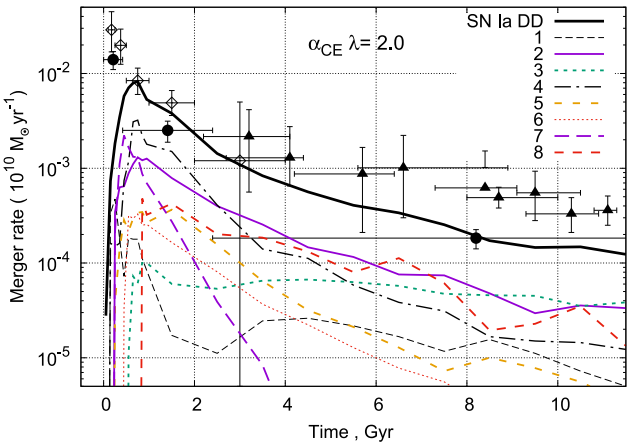

Figure 4. Delay-time distribution (DTD) for the WD mergers following the scenarios listed in Table 1 for the case $\alpha_{ce}\,\lambda = 2$. Symbols with error bars: 'observational' DTD, as in Fig. 2.

DTD for the $\alpha_{ce}\,\lambda = 2$ case, showing data for the first (0.05–2) Gyr on a log-scale. Note that, while the lines for particular scenarios are quite irregular, the summary line shows a gradual growth of the rate of SNe Ia, mainly as a result of the smooth increase of mergers occurring in zone **E** (merger of CO WDs). Recall also that at $t \lesssim$ 2 Gyr a significant contribution to the SNe Ia rate may provide a SD-channel, associated either with hydrogen or helium transfer (see e.g. Bours, Toonen & Nelemans 2013; Wang et al. 2009).

Fig. 4 shows the DTD for eight scenarios listed in Table 1 for the most prolific combination $\alpha_{ce}\,\lambda = 2$. While at very early times, $t \lesssim 1$ Gyr, scenarios 2, 4 and 7 dominate, later, at $t \approx$ (3–10) Gyr, comparable contributions are provided by scenarios 2, 3 and 8 (see also Table 3). Scenario 7 is associated with massive WDs, and there is only a very narrow 'gap' of initial separations for binaries with $M_1 \lesssim 4.5$ $M_\odot$, which just enables mergers in less than about 4 Gyr. It is important that in all scenarios one of the merging components is either a He WD or a CO WD that descended from a He star. Thus, the envelopes of WDs always have a certain amount of He, which *may* experience detonation and, under favourable conditions, trigger a detonation in an accreting WD.

As a complement to Fig. 2, in Table 3 we present the rate of WD mergers occurring at 10 Gyr after a star-formation burst in different regions of the M_{acc}–M_{don} diagram, while the rates of WD mergers at 10 Gyr after the burst as a function of $\alpha_{ce}\,\lambda$ are presented in Table 4.

Figs 1–4 and Tables 3 and 4 suggest that a satisfactory reproduction of the extant data on the DTD at $t \gtrsim$ several 100 Myr requires comparable contributions of mergers of pairs of CO+CO WDs with $M_1 + M_2 \gtrsim M_{Ch}$ and mergers of $M_1 + M_2 \lesssim M_{Ch}$ pairs with CO WD accretors and very massive He or hybrid WD donors. Basically, this agrees with the proportions of $\sim M_{Ch}$ and sub-M_{Ch} SNe Ia inferred from consideration of the solar abundance of manganese

Table 3. The rate of binary WD mergers occurring at 10 Gyr after an instantaneous star-formation burst in different regions of the M_{acc}–M_{don} diagram as a function of $\alpha_{ce}\,\lambda$ (per 10^{10} $M_\odot$ yr^{-1}). The second column indicates whether SNe Ia are potentially possible. The notation $x(y)$ means $x \times 10^y$.

Zone	DD	$\alpha_{ce}\,\lambda$			
$M_{acc} - M_{don}$	SN Ia	0.25	0.5	1.0	2.0
A	Y	4(−8) ± 4(−8)	3.7(−6) ± 5(−7)	1.3(−5) ± 1(−6)	4.9(−5) ± 2(−6)
B	Y	7(−7) ± 3(−7)	2.0(−6) ± 3(−7)	1.0(−6) ± 3(−7)	1.8(−5) ± 1(−6)
C	N	–	6.8(−8) ± 6(−8)	5.6(−6) ± 7(−7)	7.8(−6) ± 9(−7)
D	Y	–	2.3(−8) ± 3(−8)	4.1(−6) ± 6(−7)	9.5(−6) ± 9(−7)
E	Y	–	6.0(−6) ± 6(−7)	2.2(−5) ± 1(−6)	4.7(−5) ± 2(−6)
F	Y	–	7.3(−7) ± 2(−7)	1.2(−6) ± 3(−7)	5.6(−6) ± 7(−7)
G	N	–	6.3(−7) ± 2(−7)	9.7(−6) ± 1(−6)	2.2(−5) ± 1(−6)
H	N	2(−7) ± 1(−7)	–	–	1.4(−5) ± 1(−6)
I	N	2.2(−6) ± 5(−7)	8.5(−6) ± 7(−7)	1.5(−5) ± 1(−6)	4.0(−5) ± 2(−6)
J	Y	3(−7) ± 2(−7)	4.1(−6) ± 5(−7)	9.7(−6) ± 1(−6)	1.1(−5) ± 1(−6)
K	N	–	4.8(−6) ± 5(−7)	1.1(−5) ± 9(−7)	1.5(−5) ± 1(−6)
L	N	2.9(−5) ± 2(−6)	1.6(−4) ± 3(−6)	5.1(−4) ± 6(−6)	7.7(−4) ± 8(−6)
R CrB	N	3.4(−5) ± 2(−6)	2.5(−4) ± 3(−6)	4.5(−4) ± 6(−6)	5.2(−4) ± 7(−6)
SN Ia		9(−7) ± 3(−7)	1.7(−5) ± 1(−6)	5.1(−5) ± 2(−6)	1.4(−4) ± 4(−6)
WD2 Merger		6.6(−5) ± 2(−6)	4.3(−4) ± 4(−6)	1.1(−3) ± 9(−6)	1.5(−3) ± 1(−5)

Table 4. The rate of mergers of binary WDs formed via different evolutionary scenarios at 10 Gyr after an instantaneous star-formation burst as a function of $\alpha_{ce}\,\lambda$ (per $10^{10}\,M_\odot\,yr^{-1}$).

Scenario	$\alpha_{ce}\,\lambda$			
	0.25	0.5	1.0	2.0
1	–	–	–	9.8(−6) ± 2(−6)
2	–	3.9(−6) ± 7(−7)	1.3(−5) ± 2(−6)	3.6(−5) ± 4(−6)
3	9(−7)± 4(−7)	1.3(−5) ± 1(−6)	2.5(−5) ± 3(−6)	4.3(−5) ± 5(−6)
4	–	–	1.1(−5) ± 2(−6)	1.6(−5) ± 3(−6)
5	–	1.1(−7) ± 5(−8)	1.4(−6) ± 7(−7)	7.2(−6) ± 2(−6)
6	–	–	4.7(−7) ± 4(−7)	2.1(−6) ± 1(−6)
7	–	–	–	
8	–	–	–	3.1(−5) ± 4(−6)
SN Ia	9(−7)± 4(−7)	1.7(−5) ± 1(−6)	5.1(−5) ± 4(−6)	1.4(−4) ± 9(−6)

(Seitenzahl et al. 2013) and from the analysis of the mass of SNe Ia ejecta (Scalzo et al. 2014a; Scalzo, Ruiter & Sim 2014b; Childress et al. 2015); see Section 5. Note also that in the lower right panel of Fig. 2 the model results for zone **E**, namely mergers of CO+CO WD pairs with $M_1 \geq 0.8$ M$_\odot$ and $M_2 \geq 0.6$ M$_\odot$ taken alone, also fit, within errors, the observational data of Maoz et al. (2012) for the 500 Myr–2.5 Gyr and 2.5–12 Gyr time-bins.

However, mergers of sub-$M_{\rm Ch}$ pairs occur predominantly in zone **A** of the $M_{\rm acc}$–$M_{\rm don}$ diagram. Surface detonations are likely to occur only if $M_1 \gtrsim 0.8$ M$_\odot$ (Guillochon et al. 2010; Dan et al. 2012).

If the first detonation occurs in the post-merger phase, further evolution resembles that of double-detonation systems, where detonation in the envelope plays the role of the trigger, as also noted by Dan et al. (2015). For the latter scenario, it was found that, for the explosion to resemble a SN Ia, M_1 should be $\gtrsim$0.9 M$_\odot$ (Sim et al. 2010). In our simulations for $\alpha_{\rm ce}\,\lambda = 2$, in the case of an instantaneous star-formation burst, the fraction of accretors with $M_1 \gtrsim 0.8$ M$_\odot$ in the systems merging in zone **A** is, at $t \approx 10$ Gyr, close to 20 per cent. It is close to 40 per cent at $t \approx 8$ Gyr and much lower at other epochs. In the case of the SFR described by equation (4) it is permanently close to 15 per cent; see below. If the stars that do not explode in the merger process also do not explode later, the above-mentioned M_1 limits, if confirmed in the future, may strongly reduce the possible contribution of zone **A** to the rate of SN Ia.

Figs 5 and 6 illustrate the evolution with time of the distribution of masses of accretors, donors and of the total mass of the systems at merger for the case of an instantaneous star-formation burst. Fig. 6 shows these parameters for three time-bins. The average mass of accretors slightly increases with time: $M_1 \gtrsim 0.8$ M$_\odot$ have 40 per cent of accretors at (0–1) Gyr, 50 per cent at (5–6) Gyr, and 70 per cent at (10–11) Gyr. About 50 per cent of the donors have mass $\lesssim$0.6 M$_\odot$ at any epoch; the other 50 per cent are more massive. Recall that WDs with mass $\gtrsim$0.6 M$_\odot$ have only traces of He at the surface. Sub-$M_{\rm Ch}$ total mass have 60 per cent of pairs at T $\lesssim$ 6 Gyr and 40 per cent at later time. On the other hand, because the maximum mass of He WDs is close to 0.47 M$_\odot$, Fig. 5 strongly indicates that the majority of donors in merging systems are hybrid WDs.

In Fig. 7 we show the evolution of the rate of WD mergers potentially leading to SNe Ia for a galaxy mimicking the Milky Way, with the star-formation rate given by equation (4). Dependence of the rate of SNe Ia on $\alpha_{ce}\,\lambda$ for different scenarios and zones of Fig. 1 is presented in Tables 5 and 6, respectively. It is clear that, as in the case of a star-formation burst, the rate of mergers increases with $\alpha_{\rm ce}\,\lambda$, because fewer systems merge in CEs. The rate of putative SNe Ia slightly decreases with time. This reflects the decreasing rate of star formation and the fact that, in all the most prolific scenarios, mergers of DD peak at $\lesssim$1 Gyr and then decrease rather rapidly. Our estimate of the possible Galactic SNe Ia rate owing to the DD mechanism, namely 6.5×10^{-3} yr^{-1} (for the mass of the bulge and thin disc equal to 7.2×10^{10} M$_\odot$), is close to the latest estimate presented in the literature, namely $(5.4 \pm 0.12) \times 10^{-3}$ yr^{-1} (with systematic factor ∼2; Li et al. 2011). Recall, however, that we employ an extreme assumption that *all* the following contribute to SNe Ia : mergers of super-Chandrasekhar pairs of CO WD, mergers of CO WDs more massive than 0.47 $M_\odot$ with hybrid or helium WDs more massive than 0.37 $M_\odot$ and mergers of ONe and massive $\geq$0.9 $M_\odot$ CO WDs (Fig. 1). An increase of these limits will reduce the obtained rate.

The masses of accretors have a peak close to 0.7 M$_\odot$ at t =(1–7) Gyr after the beginning of star formation in the bulge and thin disc, and range predominantly between 0.45 M$_\odot$ and 1 M$_\odot$ (Fig. 8). Later, average M_1 values very smoothly become lower and

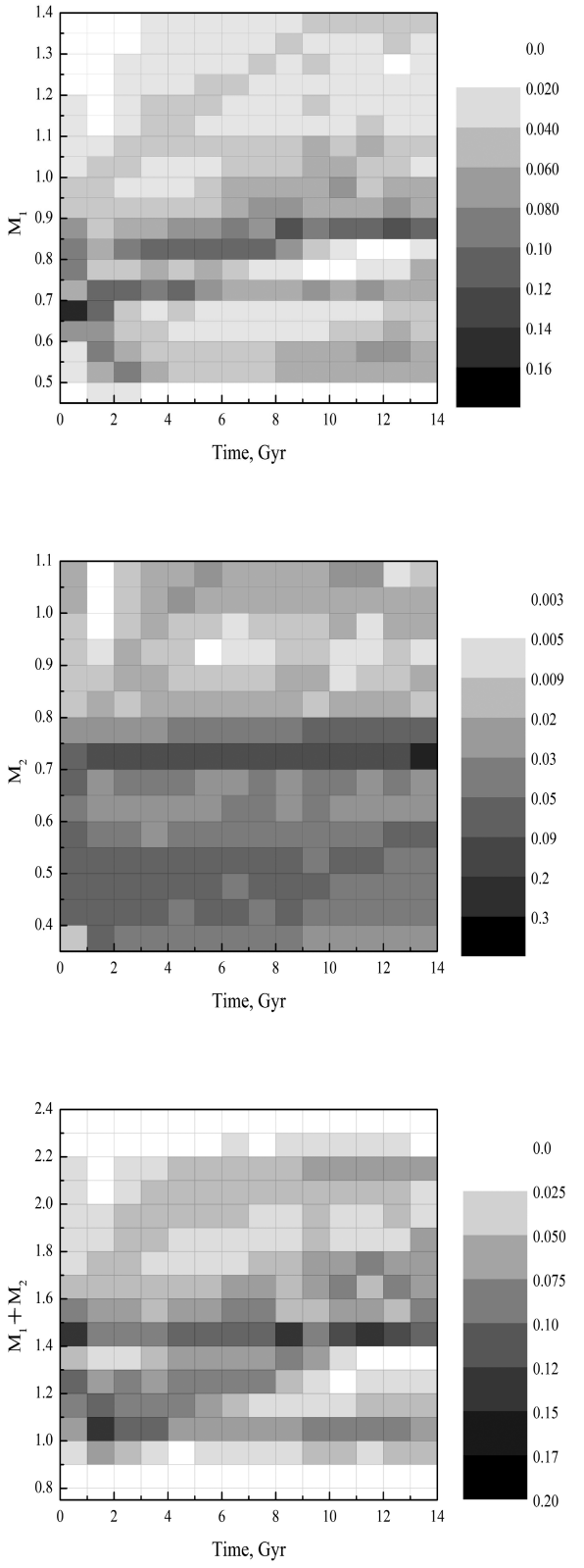

Figure 5. Distribution of masses of accretors (upper panel), donors (middle panel) and total mass (lower panel) of merging WDs versus time after an instantaneous burst of star formation. Every time-bin is normalized to 1.

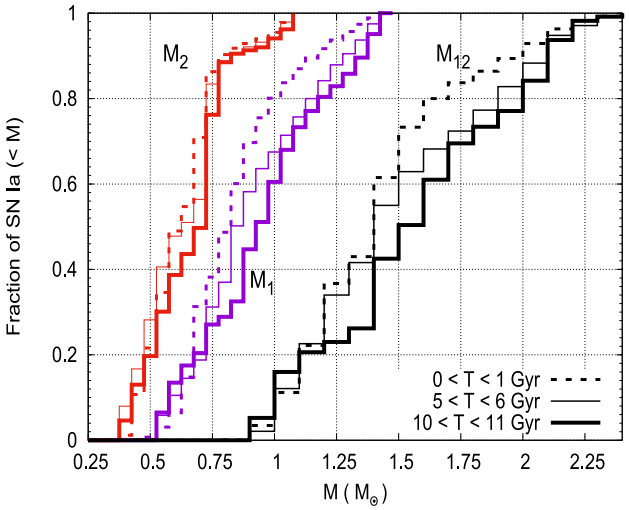

Figure 6. Distribution of M_1, M_2 and $M_1 + M_2$ (annotated as M12) at three different epochs of the evolution of the 'starburst' galaxy, shown in Fig. 5. Dotted lines, $0 \le t \le 1$ Gyr; thin solid lines, $5 \le t \le 6$ Gyr; thick solid lines, $10 \le t \le 11$ Gyr.

at the current assumed age of the Galaxy (14 Gyr) most of the accretor masses are between 0.6 and 1.0 $M_\odot$. Donor masses have two peaks – close to 0.7 $M_\odot$ (CO WD) and at 0.4 $M_\odot$ to 0.6 $M_\odot$ (most massive He WDs and hybrid WDs). The existence of two peaks in donor masses results in a double-peaked distribution of the total mass of merging WDs, with peaks close to 1.0 $M_\odot$and 1.4 $M_\odot$.

5 DISCUSSION

5.1 Tidal effects

A substantial uncertainty in the results of BPS for putative precursors of SNe Ia is caused by the treatment of tidal effects. As noted in Section 3.1, they are not always taken into account, in contrast to our study. In order to illustrate the effect of tides, in Fig. 9 we present a model DTD obtained using the same BPS code, but excluding tidal effects, and compare it with the model DTD obtained 'with tides' and with observations, as in Fig. 2. We present only summary curves. It is immediately clear that in the extreme case of the absence of tides, the DTD becomes more compatible with observations, at least for the DTD derived from SNe Ia in the Subaru/*XMM* Survey by Totani et al. (2008) (diamonds) and in galaxy clusters by Maoz et al. (2010) (triangles). For comparison, we also show that, if as an extreme assumption we suppose that *all* merging WDs produce SNe Ia, the rate of the latter owing to the DD scenario becomes even higher than observed. The reason for better agreement with observations may be understood as the effect of typically later RLOF in the same systems and the production of more massive WDs. Some systems experience case C of mass exchange instead of case B.

5.2 Metallicity

Another source of uncertainty is stars with subsolar metallicity: $Z \sim 0.0001$ may be typical for the first generation of stars enriched by heavy elements produced in explosions of Population III stars (Smith et al. 2015). Even in the Galaxy, about 10 ultra-low-metallicity ([Fe/H] < -7) stars are known (Keller et al. 2014). The

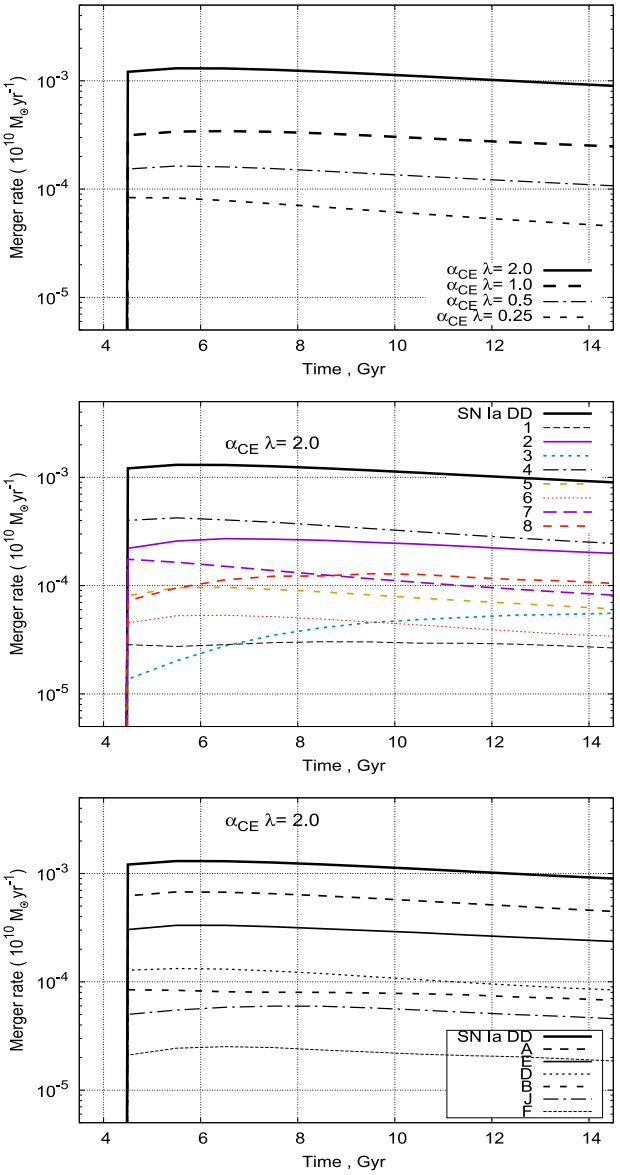

Figure 7. Evolution of the rate of WD mergers potentially leading to SNe Ia in the Galaxy, if the star-formation rate is set by equation (4). Upper panel, all potential SNe Ia as a function of $\alpha_{ce}\,\lambda$. Middle panel, systems produced by particular scenarios (Table 1). Lower panel, systems feeding different regions of the M_{acc}–M_{don} diagram (Fig. 1).

Table 5. The rate of mergers of binary WDs resulting in SNe Ia formed via different evolutionary channels at t =14 Gyr as a function of $\alpha_{ce}\,\lambda$ (per $10^{10}\,M_\odot\,yr^{-1}$). The star-formation rate follows equation (4). The errors are negligibly small compared with rates.

Scenario	$\alpha_{ce}\,\lambda$			
	0.25	0.5	1.0	2.0
1	–	5.3(−7)	9.0(−6)	2.8(−5)
2	2.9(−6)	2.1(−5)	7.2(−5)	2.1(−4)
3	4.3(−5)	9.9(−5)	9.2(−5)	5.5(−5)
4	2.4(−7)	1.8(−6)	5.5(−5)	2.6(−4)
5	4.7(−8)	1.3(−6)	1.2(−5)	6.3(−5)
6	–	3.1(−7)	9.1(−6)	3.5(−5)
7	–	–	–	8.5(−5)
8	–	–	9.7(−7)	1.1(−4)
SN Ia	4.7(−5)	1.2(−4)	2.5(−4)	9.0(−4)

Table 6. The rate of mergers of binary WDs resulting in SNe Ia formed via different evolutionary channels and occurring in different regions of the $M_{\rm acc}$–$M_{\rm don}$ diagram at t =14 Gyr as a function of $\alpha_{\rm ce}\,\lambda$ (per $10^{10}\,{\rm M}_{\odot}{\rm yr}^{-1}$). The star-formation rate follows equation (4). Row 'SN Ia' provides the rate of potential SN Ia, while row 'WD2' shows the total rate of WD mergers.

Zone	DD	$\alpha_{\rm ce}\,\lambda$			
$M_{\rm acc} - M_{\rm don}$	SN Ia	0.25	0.5	1.0	2.0
A	Y	1.5(−5)	5.7(−5)	1.0(−4)	4.5(−4)
B	Y	5.8(−6)	3.9(−6)	1.1(−5)	6.8(−5)
C	N	1.4(−6)	1.3(−5)	3.2(−5)	8.4(−5)
D	Y	6.4(−7)	5.2(−6)	2.0(−5)	8.4(−5)
E	Y	1.8(−5)	3.1(−5)	9.1(−5)	2.4(−4)
F	Y	5.6(−7)	1.2(−6)	3.0(−6)	1.9(−5)
G	N	8.2(−9)	5.9(−6)	5.5(−5)	5.7(−5)
H	N	1.2(−7)	1.3(−7)	7.7(−7)	3.9(−5)
I	N	1.1(−5)	3.3(−5)	6.4(−5)	1.3(−4)
J	Y	5.2(−6)	9.1(−6)	2.2(−5)	4.6(−5)
K	N	4.8(−6)	2.6(−5)	4.4(−5)	4.4(−5)
L	N	9.7(−5)	2.2(−4)	6.4(−4)	1.0(−3)
R CrB	N	4.7(−5)	4.6(−4)	1.4(−3)	1.7(−3)
SN Ia		4.7(−5)	1.2(−4)	2.5(−4)	9.0(−4)
WD2		2.1(−4)	8.6(−4)	2.4(−3)	4.0(−3)

reduction of Z to an extreme value of 0.0001 results in an improvement of agreement with observational DTDs (Fig. 2). The reason is a general increase of the pre-contact masses of stars with decreasing Z, owing to strongly reduced stellar winds. However, this result should be taken with a pinch of salt: the evolution of close binaries with non-solar Z in all BPS codes is an extrapolation of computations for Z = 0.02. Because of the different masses of stellar remnants at the end of similar evolutionary stages, the time-scales of evolution, further evolutionary scenarios and/or their relative significance may be different. In addition, the chemical composition of WDs depends on their initial metallicity and may influence the development of explosions involving them.

5.3 Stability of mass loss by the donors

A long-standing problem is the stability of mass loss by donors with deep convective envelopes and in systems with components with a high mass-ratio. In simulations, we used critical values of the mass-ratios of components for low-mass stars and giants implemented in BSE (Hurley et al. 2002, equations 56, 57), thus allowing stable mass loss by stars with deep convective envelopes only for $q_{\rm cr} = M_{\rm don}/M_{\rm acc} \lesssim 1$, even if the donor has a condensed core. However, recent studies (Woods & Ivanova 2011; Passy, Herwig & Paxton 2012) have shown that dynamical mass loss by red giants may be avoided owing to the existence of a super-adiabatic outer layer of the giant's envelope, which has a local thermal time-scale comparable to the dynamical time-scale and enough time to readjust thermally. Pavlovskii & Ivanova (2015) found that $q_{\rm cr}$ varies from 1.5 to 2.2 for conservative mass transfer.[5] In scenarios 1–4 (Table 1), the first CO WD in the system forms via stable RLOF. For a revised upward $q_{\rm cr}$, more systems would avoid the first CE and, possibly, evolve to form a pair of WDs. Because typical separations of components after the second CE will be larger, a lower efficiency of matter ejection in CEs will be required for retaining or increasing the rate of WD mergers.

[5] Earlier, the possibility of $q_{\rm cr} \simeq 2$ was found by Chen & Han (2008) in evolutionary computations, but no physical justification was provided.

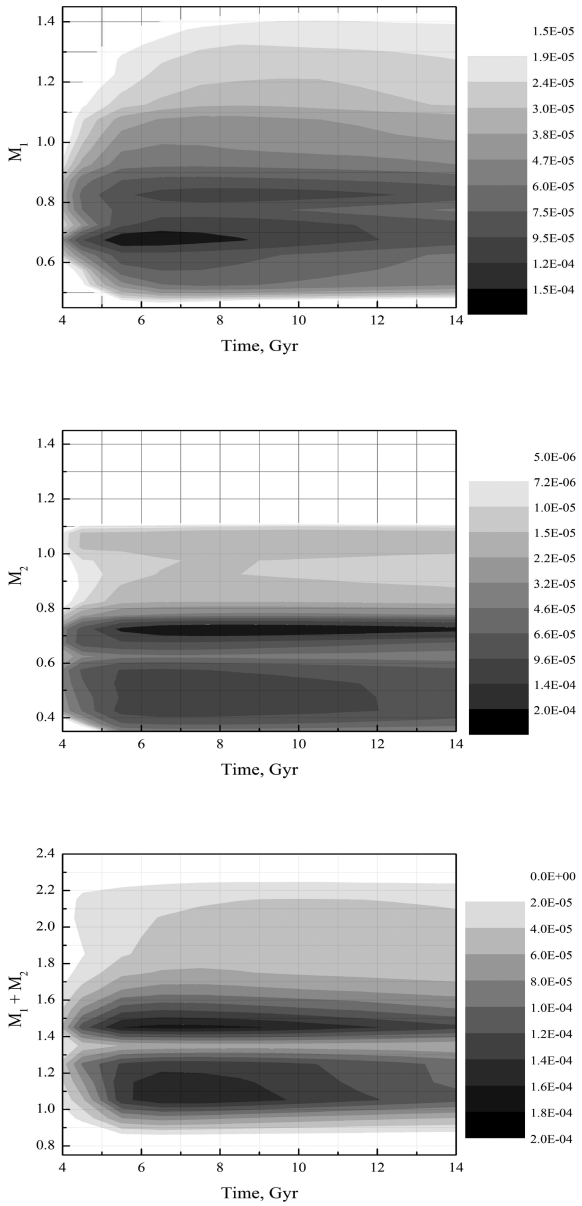

Figure 8. Distribution of masses of accretors (upper panel), donors (middle panel) and total mass (lower panel) of merging pairs of WDs potentially leading to SNe Ia versus time for a 10^{10} M$_{\odot}$ galaxy with the star-formation rate set by equation (4).

5.4 Pre-CE core radii of the donors

Hall & Tout (2014) called attention to an uncertainty inherent in *all* BPS codes: it is unclear what values of radii it is necessary to compare in order to find whether stars merged in CEs, namely the pre-CE core radii of the donors or the radii of post-CE stripped remnants. Currently, in BSE the first option is implemented. Furthermore, the radii of the stellar cores themselves are poorly approximated. This uncertainty may influence, mostly, the outcome of the CE produced by RLOF in the pairs of (i) HG and RGB stars, (ii) RGB and RGB stars, and (iii) in binaries harbouring HG or RGB stars with He WD companions. In order to test the suggestion of Hall & Tout (2014), we implemented corrections in the code suggested by them for RGB and TPAGB stars. However, in our simulations we did not encounter events of the kinds (i) and (ii), while CEs with He WD are rare. Thus, our results remained virtually unaffected. The

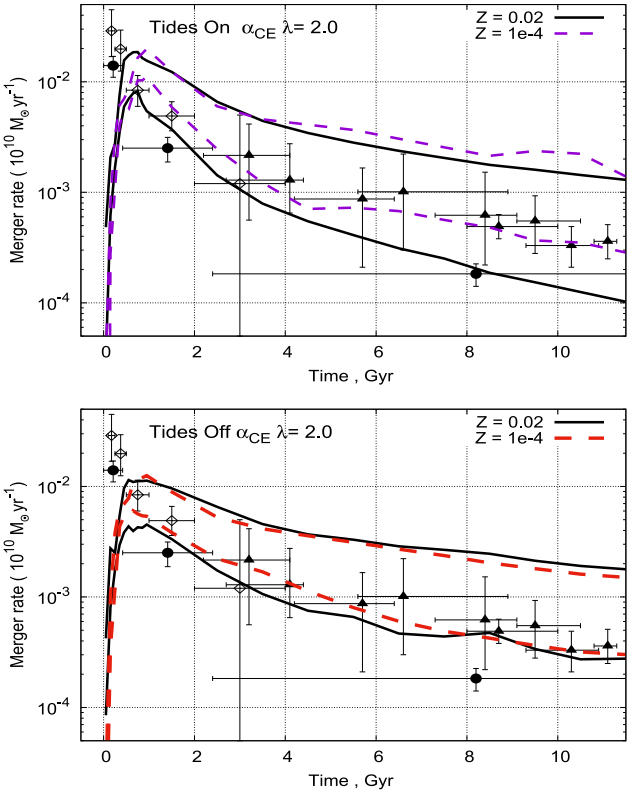

Figure 9. The effect of tides and the abundance of metals on the delay-time distribution (DTD). Upper panel: lower solid line, DTD in the 'standard' model for $\alpha_{ce}\,\lambda = 2$, $Z = 0.02$ with tides taken into account; lower dashed line, DTD computed in the same model for $Z = 0.0001$. The upper pair of lines shows the DTD for the merger of *all* WDs for two values of Z. Lower panel: the same distributions for the case when tidal effects are not taken into account. Observational data points are the same as in Fig. 2.

above-mentioned imperfections are partially offset by uncertainties in the core–envelope definition (i.e. envelope binding energy) and CE ejection efficiency. Hall & Tout (2014) noted that it is difficult to constrain the parameters found by them to be uncertain by observations, as the spatial densities of the binaries concerned are poorly known. All the above-mentioned problems in the treatment of binary star evolution require a more systematic investigation before it will be possible to quantify the respective effects to a degree that will allow us to make the necessary corrections in BPS codes. It is impossible to evaluate the influence of all of them on the rate of formation of putative progenitors of SNe Ia, but it may be suspected that, for example, the rates of merger of WDs will change within a factor of 2–3.

5.5 The slope of the DTD curve

The slope of the DTD curve versus the time close to t^{-1} is often considered as evidence in favour of the DD scenario being the main mechanism producing SNe Ia. If the distance between the components a after the last CE episode obeys the power law $\mathrm{d}N/\mathrm{d}a \propto a^{\epsilon}$, while the merger time depends on a as $t \propto a^{\gamma}$, the dependence of the DTD on time should be a power law with index $\phi = -1 + (\epsilon + 1)/\gamma$. It is usually *assumed* that merging pairs of WDs are distributed over a like main sequence stars. Then $\phi = -1$ by virtue of the almost 'standard' assumption $\epsilon = -1$ (Popova, Tutukov & Yungelson 1982). In Fig. 10, we show the distribution of progenitors

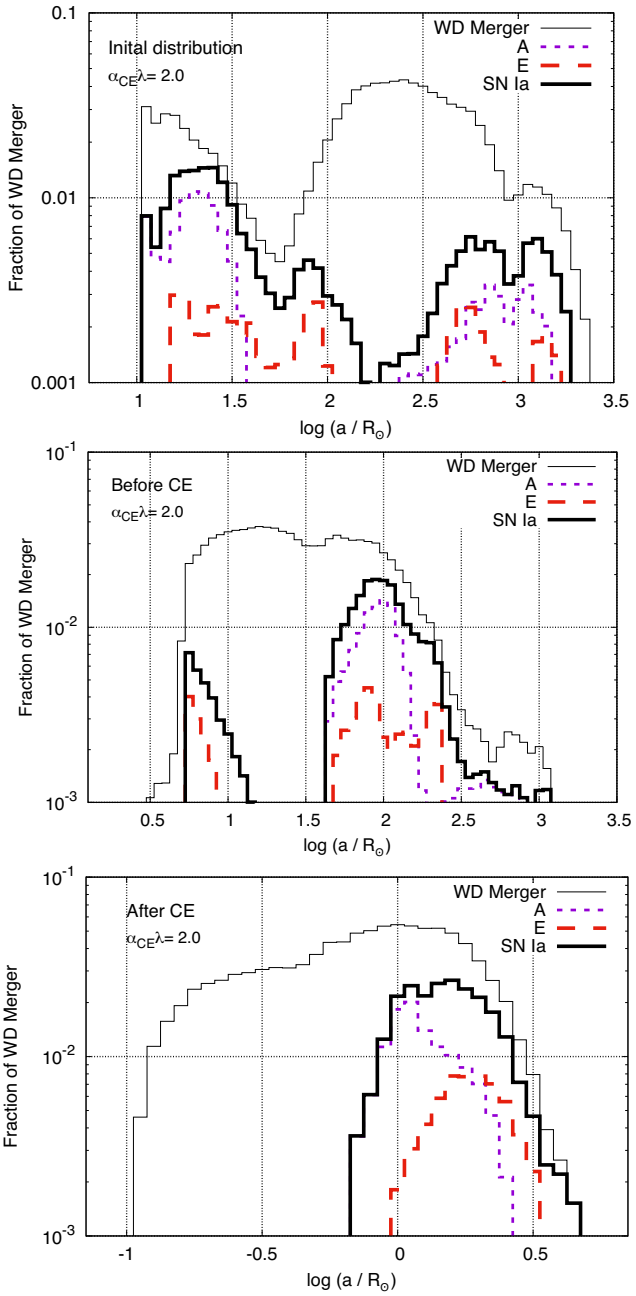

Figure 10. Distribution of separations of components of precursors of merging white dwarf (WD) pairs, $\mathrm{d}N/\mathrm{dlog}\,(a)$. The distribution is normalized to the total number of WDs that merged over 10 Gyr (WD Merger in the legend). Upper panel, initial distribution. Middle panel, distribution before the last common envelope (CE) stage. Lower panel, distribution after the last CE.

of merging WD+WD binaries on the main sequence and before and after the last CE episode. It is clear that, in the course of evolution distribution over, a experiences a complicated non-linear transformation and, separately, neither sub-$M_{\rm Ch}$ nor (super)-$M_{\rm Ch}$ mergers obey a a^{-1} law, but the latter is, crudely, followed by their combination. If other mechanisms also contribute to SNe Ia, they may also influence the slope of the DTD curve. The disagreement between the shape of the model time dependence of merging double-degenerates and a simple power-law was also noted by Ablimit, Maeda & Li (2016).

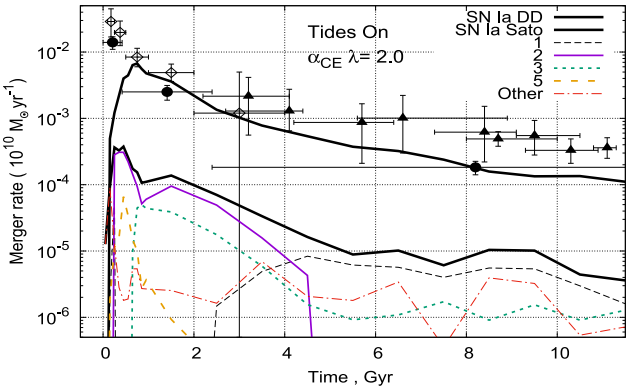

Figure 11. Comparison of the observational DTD with the model distribution for systems obeying equation (1). Upper solid line, delay-time distribution (DTD) in the 'standard' model. Lower sold line, DTD for mergers of WD satisfying equation (1). The rest of the lines show the contributions of particular scenarios, as in Fig. 4.

5.6 The rate of SNe Ia

The aim of our study was to estimate the upper bound to the input of mergers of WDs into the rate of SNe Ia. For a satisfactory agreement with observations, at least some of the included model events should be sub-$M_{\rm Ch}$ mergers, involving CO accretors and massive He and hybrid (COHe) donors. Observations provide some evidence in favour of the existence of sub-$M_{\rm Ch}$ SNe Ia, through a significant scatter in the estimated masses of produced ^{56}Ni and ejected mass, which for some samples cluster around certain values substantially below $M_{\rm Ch}$ (e.g. Stritzinger et al. 2006; Mazzali et al. 2007; Scalzo et al. 2014a,b; Childress et al. 2015). In particular, Scalzo et al. (2014a,b) claim that the fraction of sub-$M_{\rm Ch}$ SNe Ia may be up to 50 per cent. However, as yet, no conclusions have been drawn regarding whether these features of SNe Ia are related to their mass or to variations in the explosion conditions of $M_{\rm Ch}$ WDs. On the other hand, our model sample of merging pairs of WDs contains a substantial fraction of strongly super-$M_{\rm Ch}$ pairs. As shown by Moll et al. (2013), however, the spectra of SNe Ia produced in these events resemble the spectra of 'normal' SNe Ia.

We noted in comments to Figs 2 and 4 that, within observational errors, we obtain satisfactory agreement with observations even if we assume that only CO+CO WD pairs with $M_1 \geq 0.8$ M$_\odot$ and $M_2 \geq 0.6$ M$_\odot$ can produce SNe Ia. Here, we implicitly assumed that SNe Ia may explode either in the merger stage or in the merger product evolution stage. This issue is, however, still open. If we assume that exploding pairs in which explosion conditions are met occur in the merger stage only and that equation (1) should be satisfied, the expected rate of SNe Ia drops sharply. In Fig. 11, we compare the observational DTD with the model distribution for systems obeying equation (1). A reduction of the rate by a factor of ∼20 at t =10 Gyr is immediately seen. This may signify serious problems either with observational estimates of the DTD or in our understanding of the processes that occur during and after mergers. It is interesting that scenario 3, which is one of the main contributors to the SNe Ia rate in the 'standard' model, in the 'Sato et al.' case terminates the production of massive mergers after ∼4 Gyr.

6 CONCLUSION

In the present study we have attempted to estimate the maximum possible contribution of merging binary WDs to the total rate of SNe Ia. The main motivation of the study was the fact that, currently, the merger of WDs is the only known (but still hypothetical) mechanism that has a natural time-scale overlapping with Hubble time. In our study we did not consider the relations between different types of SNe Ia and possible combinations of the components of the merging pairs, as we recognize that there are 'grey zones' in which current simulations of mergers do not demonstrate events that are similar to SNe Ia of any known kind. This may be related to the inaccessibility of the physical conditions necessary for SNe Ia explosions or be a result of an inadequate understanding of the physics, or of numerical problems. The only limits imposed on the components of merging pairs arose from the knowledge that merger results at least in a single detonation, which may be treated as a transient event.

We found the most common scenarios of close binary star evolution that result in the formation of merging pairs of WDs and studied the dependence of their relative role on the still cryptic parameters of the binding energy of stellar envelopes (λ) and the efficiency of the expulsion of matter in the CE stages ($\alpha_{\rm ce}$). We parametrized scenarios by a product $\alpha_{\rm ce}$ λ, which we varied from 0.25 to 2.0. We found, in agreement with some earlier studies (e.g. Mennekens et al. 2010; Toonen et al. 2012; Ruiter et al. 2013; Claeys et al. 2014), that most merging pairs have a stable RLOF as the first stage of mass transfer. At low $\alpha_{\rm ce}$ λ the dominant scenarios are those in which the first RLOF occurs when the primary star overflows the Roche lobe in the Hertzsprung gap or in the red giant stage. For larger $\alpha_{\rm ce}$ λ, scenarios in which the first RLOF occurs in the EAGB or TPAGB stages start to play role. It is important that in about 50 per cent of merging pairs of WDs at least one of the components is a He or a hybrid CO WD. The latter, in fact, dominate. The presence of at least traces of He at the surface of WDs may facilitate explosion at merger. With an increase of $\alpha_{\rm ce}$ λ, the roles of different scenarios become more even.

With an increase of $\alpha_{\rm ce}$ λ from 0.25 to 2, the total rate of mergers increases. If $\alpha_{\rm ce}$ λ is low, a large fraction of systems merges in CE. If this product of model parameters is high, significant fraction of WD+WD pairs is too wide to merge in Hubble time.

We compared the model DTD with results derived from observations of several samples of SNe Ia. In the model, we considered the mergers singled out in the $M_{\rm acc}$–$M_{\rm don}$ diagram as precursors of SNe Ia. The best agreement with observations was obtained for high $\alpha_{\rm ce}$ λ = 2. Within observational errors, at $1 \lesssim t \lesssim 8$ Gyr, the model DTD for all mergers agrees with the DTD derived by Totani et al. (2008) and Maoz et al. (2010, 2012). For earlier epochs, the model DTD has about 3 times fewer events. For $t \approx 10$ Gyr, the discrepancy with the data of Maoz et al. (2012) is by a factor ∼4. If we take into account only 'canonical' mergers of CO+CO WDs with $M_1 + M_2 \geq 1.4$, the model DTD still is roughly comparable with the lowest observational DTD estimates for field galaxies (Maoz et al. 2012), as in the studies of Ruiter et al. (2013) and Claeys et al. (2014),[6] but SNe Ia rates are higher than in the models of Ablimit et al. (2016), in which a more stringent requirement, $M_1 + M_2 \geq 1.6$ M$_\odot$, $q > 0.8$, is applied. The current rate of SNe Ia in the Milky Way, if all mergers expected by us to result in SNe Ia of some kind really produce them, is 6.5×10^{-3} yr^{-1}, which is remarkably close to the observationally inferred estimate of $(5.4 \pm 0.12) \times 10^{-3}$ yr^{-1}.

[6] Actually, this is not surprising, because the codes used by Toonen et al. (2012), Ruiter et al. (2013) and Claeys et al. (2014) are based on the same system of evolutionary tracks as the BSE code; the difference between the codes is, as mentioned in the text, in the treatment of the evolution of binaries (Toonen et al. 2014).

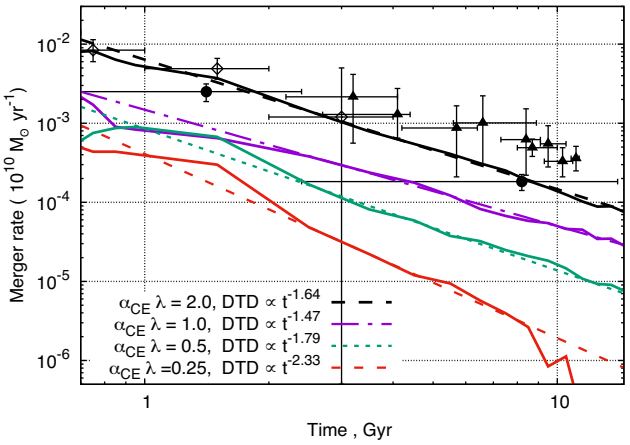

Figure 12. The slope of the delay-time distribution (DTD) for $t \geq 1$ Gyr, as in Fig. 2. Tides are accounted in the model, Z = 0. 2. Solid lines show model results. Broken lines represent power-law approximations to the DTD for different values of $\alpha_{ce}\,\lambda$.

The model estimate may be lower if our equation (4) overestimates the actual Galactic SFR (see e.g. Chomiuk & Povich 2011).

The transformations of the separation of components during evolution with RLOF and CEs are strongly non-linear. Different scenarios produce non-flat distributions over $\log(a)$ and their sum is also not flat. As a result, we find that the model DTD does not depend on time like a power law with an exponent close to -1, as expected from simplified estimates, assuming that after the last CE episode the distribution of separations of WD is flat in $\log(a)$. The slope of DTD in our models is a power law, depending on the assumed $\alpha_{ce}\,\lambda$ (Fig. 12). The exponents of the power law range from -2.35 to -1.64 for $\alpha_{ce}\,\lambda$ from 0.25 to 2, respectively. The curve with the smallest absolute value of the exponent fits observations for $t \lesssim 8$ Gyr.

Our model does not fit the Maoz et al. (2012) bin of DTD at the shortest delay, namely $t \lesssim 420$ Myr. However, most SNe Ia in this time-bin may actually be produced by double-detonations. It was shown by Ruiter et al. (2014) that the double-detonation scenario involving non-degenerate donors and massive CO WD accretors reaches a peak at 200–300 Myr and extends to about 500 Myr. At the peak, the rate of SNe Ia is $(3-4)\times10^{-3}$ per $10^{10}\,M_\odot\,yr^{-1}$. The DTD of Ruiter et al. (2014) has a second peak, comparable in maximum rate and extending to several Gyr. It is produced by the systems with long-living degenerate He donors (AM CVn stars). However, it was shown by Piersanti et al. (2015) that in such systems outbursts of He burning never become dynamical and, respectively, AM CVn stars with He dwarf donors produce neither 'regular' SNe Ia nor lower-scale SNe .Ia. Thus, this scenario cannot play any role in early-type galaxies with the majority of stars formed in the initial spike of star formation. For the earliest epochs, inclusion of both SNe Ia of double-degenerate origin and double-detonation SNe Ia may reduce the discrepancy between observations and model.

Some evidence in favour of the existence of sub-M_{Ch} SNe Ia is not related directly to the interpretation of their observations. As noted above, Seitenzahl et al. (2013) noticed that manganese is produced efficiently in explosions only of WDs close to M_{Ch}. The observed [Mn/Fe] ratio in the solar neighbourhood may be reproduced if about half of SNe Ia involve near-M_{Ch} WDs, while the rest may be sub-M_{Ch}. However, this conclusion does not restrict the mechanism of sub-M_{Ch} SNe Ia. Badenes & Maoz (2012) estimated the merger rate of Galactic binary WDs and found that it is rather similar to the inferred rate of SNe Ia in Milky Way-like Sbc galaxies. They concluded that there are not nearly enough super-M_{Ch} pairs of WDs to reproduce this rate and, therefore, sub-M_{Ch} pairs may be partially responsible for the SNe Ia rate.

One prediction of single-degenerate models with non-degenerate donors is the sweeping of H- or He-rich material from the envelope of the donor by the SN ejecta. To date, 17 'normal' SNe Ia have been surveyed for swept-up matter. The upper limits on the amount of the latter are inconsistent with a MS/RG donor (see Maguire et al. 2016, and references therein). On the other hand, as noted by Shen, Guillochon & Foley (2013), nascent He WDs have thin H envelopes, which, in the case of merging WDs, will be transferred stably onto the CO accretor prior to tidal disruption of the He core of the donor. This hydrogen is likely to be ejected from the binary in nova eruptions and to sweep up the surrounding interstellar medium (ISM) hundreds to thousands of years prior to a possible SN Ia. As found by Shen et al. (2014), this may create ISM profiles closely matching those inferred from the observations of some SNe Ia. In addition, the interaction of tidal tails with the ISM may create Na I D-line profiles similar to those observed (Raskin & Kasen 2013). Thus, observations of narrow absorption lines from circumstellar medium do not necessarily manifest the presence of a non-degenerate component in a pre-SN Ia binary.

On the other hand, the existence of a single-degenerate (SD) channel to SN Ia may be signified by the enhanced brightness and blue and ultraviolet emission arising when the ejected material interacts with the companion star (Kasen 2010). UV-emission bursts were recently observed in the early spectra of several SNe Ia (Cao et al. 2015; Im et al. 2015; Marion et al. 2016). However, the interpretation of their observations as a manifestation of a SD scenario is still a matter of debate (Liu & Stancliffe 2016; Kromer et al. 2016). For a variety of SD scenarios – SNe Ia in symbiotic systems – Chomiuk et al. (2016), based on radio observations, limit the fraction of SNe Ia in systems with red giant components to $\lesssim$10 per cent. Strong evidence for Chandrasekhar-mass explosions is provided by observations of SN remnant 3C 397 (Yamaguchi et al. 2015), for which the Ni/Fe and Mn/Fe mass ratios derived from X-ray observations are consistent only with nucleosynthesis processes occurring in a near-M_{Ch} SN.

It would be incorrect to blame population synthesis alone for the mismatch of models and observations. As noted in Section 2, SPH simulations of merger processes suffer from insufficient resolution. An increase in resolution will allow us to resolve smaller hot regions, thus allowing a better understanding of the conditions for detonation at contact, especially in systems with He-rich donors. DTD, in turn, are uncertain by almost an order of magnitude, as seen in the figures above; almost certainly this is not an effect of the different methods applied for their recovery, but also an effect of the dependence of the samples of SNe Ia under study on the environment.

We have shown that by accounting for all WD merger events that hypothetically *may* produce SNe Ia either during merger processes or in the course of further evolution, it is possible within reasonable limits to explain the DTD for SNe Ia and the rate of SNe Ia in the Milky Way. However, the diversity of the combinations of the chemical composition of the components of merging pairs and their masses leaves open the question why the majority of SNe Ia are so 'standard'.

ACKNOWLEDGEMENTS

The authors acknowledge the referee for his/her valuable comments. We appreciate helpful discussions with M. Dan, N. Chugai,

G. Nelemans, K. Postnov, S. Toonen and H.-L. Chen. D. Kolesnikov is acknowledged for trial computations of evolutionary sequences for helium stars. We acknowledge J. Hurley and his co-authors for making the code BSE public. LRY was partially supported by Basic Research Program P-7 of the Praesidium of the Russian Academy of Sciences and Russian Foundation for Basic Research (contract no. 14-02-00604). AGK acknowledges support from Russian Science Foundation grant 14-12-00146 and the M.V. Lomonosov Moscow State University Program of Development. This research made use of NASA's ADS Bibliographic Services.

REFERENCES

Ablimit I., Maeda K., Li X.-D., 2016, ApJ, 826, 53
Badenes C., Maoz D., 2012, ApJ, 749, L11
Bours M. C. P., Toonen S., Nelemans G., 2013, A&A, 552, 24
Brooks J., Bildsten L., Marchant P., Paxton B., 2015, ApJ, 807, 74
Bulla M., Sim S. A., Pakmor R., Kromer M., Taubenberger S., Röpke F. K., Hillebrandt W., Seitenzahl I. R., 2016, MNRAS, 455, 1060
Burkart J., Quataert E., Arras P., Weinberg N. N., 2013, MNRAS, 433, 332
Camacho J., Torres S., García-Berro E., Zorotovic M., Schreiber M. R., Rebassa-Mansergas A., Nebot Gómez-Morán A., Gänsicke B. T., 2014, A&A, 566, 86
Cao Y. et al., 2015, Nature, 521, 328
Chen X., Han Z., 2002, MNRAS, 335, 948
Chen X., Han Z., 2008, MNRAS, 387, 1416
Childress M. J. et al., 2015, MNRAS, 454, 3816
Chomiuk L., Povich M. S., 2011, AJ, 142, 197
Chomiuk L. et al., 2016, ApJ, 821, 119
Claeys J. S. W., Pols O. R., Izzard R. G., Vink J., Verbunt F. W. M., 2014, A&A, 563, 83
D'Souza M., Motl P., Tohline J. J. F., 2006, ApJ, 643, 381
Dan M., Rosswog S., Brüggen M., 2009, J. Phys. Conf. Ser., 172, 012034
Dan M., Rosswog S., Guillochon J., Ramirez-Ruiz E., 2011, ApJ, 737, 89
Dan M., Rosswog S., Guillochon J., Ramirez-Ruiz E., 2012, MNRAS, 422, 2417
Dan M., Rosswog S., Brüggen M., Podsiadlowski P., 2014, MNRAS, 438, 14
Dan M., Guillochon J., Brüggen M., Ramirez-Ruiz E., Rosswog S., 2015, MNRAS, 454, 4411
de Kool M., 1990, ApJ, 358, 189
Dubey A., Reid L. B., Weide K., Antypas K., Ganapathy M. K., Riley K., Sheeler D., Siegal A., 2009, preprint (arXiv:0903.4875)
Fryxell B. et al., 2000, ApJS, 131, 273
Fuller J., Lai D., 2012, MNRAS, 421, 426
Gilmore G., 2001, in Funes J. G., Corsini E. M., eds, Astronomical Society of the Pacific Conference Series Vol. 230, Galaxy Disks and Disk Galaxies. Astron. Soc. Pac., San Francisco, p. 3
Guerrero J., García-Berro E., Isern J., 2004, A&A, 413, 257
Guillochon J., Dan M., Ramirez-Ruiz E., Rosswog S., 2010, ApJ, 709, L64
Hall P. D., Tout C. A., 2014, MNRAS, 444, 3209
Hillebrandt W., Kromer M., Röpke F. K., Ruiter A. J., 2013, Frontiers Phys., 8, 116
Holcomb C., Guillochon J., De Colle F., Ramirez-Ruiz E., 2013, ApJ, 771, 14
Hoyle F., Fowler W. A., 1960, ApJ, 132, 565
Hurley J. R., Pols O. R., Tout C. A., 2000, MNRAS, 315, 543
Hurley J. R., Tout C. A., Pols O. R., 2002, MNRAS, 329, 897
Hut P., 1981, A&A, 99, 126
Iben I. J., 1986, ApJ, 304, 201
Iben I., Tutukov A. V., 1984, ApJS, 54, 335
Iben I., Tutukov A. V., 1985, ApJS, 58, 661
Iben I. J., Tutukov A. V., 1991, ApJ, 370, 615
Iben I. J., Tutukov A. V., Yungelson L. R., 1996, ApJ, 456, 750
Ilkov M., Soker N., 2012, MNRAS, 419, 1695
Im M., Choi C., Yoon S.-C., Kim J.-W., Ehgamberdiev S. A., Monard L. A. G., Sung H.-I., 2015, ApJS, 221, 22
Ivanova N. et al., 2013, A&AR, 21, 59
Ji S. et al., 2013, ApJ, 773, 136
Jorgensen H. E., Lipunov V. M., Panchenko I. E., Postnov K. A., Prokhorov M. E., 1997, ApJ, 486, 110
Kasen D., 2010, ApJ, 708, 1025
Kashi A., Soker N., 2011, MNRAS, 417, 1466
Kashyap R., Fisher R., García-Berro E., Aznar-Siguán G., Ji S., Lorén-Aguilar P., 2015, ApJ, 800, L7
Katz M. P., Zingale M., Calder A. C., Swesty F. D., Almgren A. S., Zhang W., 2016, ApJ, 819, 94
Keller S. C. et al., 2014, Nature, 506, 463
Kiel P. D., Hurley J. R., Bailes M., Murray J. R., 2008, MNRAS, 388, 393
Kitaura F. S., Janka H.-T., Hillebrandt W., 2006, A&A, 450, 345
Klypin A., Zhao H., Somerville R. S., 2002, ApJ, 573, 597
Kromer M. et al., 2016, MNRAS, 459, 4428
Levanon N., Soker N., García-Berro E., 2015, MNRAS, 447, 2803
Li W., Chornock R., Leaman J., Filippenko A. V., Poznanski D., Wang X., Ganeshalingam M., Mannucci F., 2011, MNRAS, 412, 1473
Liu Z.-W., Stancliffe R. J., 2016, MNRAS, 459, 1781
Livne E., Glasner A., 1991, ApJ, 370, 272
McKernan B., Ford K. E. S., 2016, MNRAS,
Maguire K., Taubenberger S., Sullivan M., Mazzali P. A., 2016, MNRAS, 457, 3254
Maoz D., Sharon K., Gal-Yam A., 2010, ApJ, 722, 1879
Maoz D., Mannucci F., Brandt T. D., 2012, MNRAS, 426, 3282
Maoz D., Mannucci F., Nelemans G., 2014, ARA&A, 52, 107
Marion G. H. et al., 2016, ApJ, 820, 92
Marquardt K. S., Sim S. A., Ruiter A. J., Seitenzahl I. R., Ohlmann S. T., Kromer M., Pakmor R., Röpke F. K., 2015, A&A, 580, A118
Marsh T. R., Nelemans G., Steeghs D., 2004, MNRAS, 350, 113
Mazzali P. A., Röpke F. K., Benetti S., Hillebrandt W., 2007, Science, 315, 825
Mennekens N., Vanbeveren D., De Greve J. P., De Donder E., 2010, A&A, 515, 89
Moll R., Raskin C., Kasen D., Woosley S. E., 2014, ApJ, 785, 105
Nelemans G., Yungelson L. R., Portegies Zwart S. F., Verbunt F., 2001a, A&A, 365, 491
Nelemans G., Portegies Zwart S. F., Verbunt F., Yungelson L. R., 2001b, A&A, 368, 939
Nomoto K., 1982, ApJ, 257, 780
Ohlmann S. T., Röpke F. K., Pakmor R., Springel V., 2016, ApJ, 816, L9
Paczyński B., 1971, Acta Astron., 21, 1
Pakmor R., Kromer M., Röpke F. K., Sim S. A., Ruiter A. J., Hillebrandt W., 2010, Nature, 463, 61
Pakmor R., Kromer M., Taubenberger S., Sim S. A., Röpke F. K., Hillebrandt W., 2012, ApJ, 747, L10
Pakmor R., Kromer M., Taubenberger S., Springel V., 2013, ApJ, 770, L8
Passy J.-C., Herwig F., Paxton B., 2012, ApJ, 760, 90
Pavlovskii K., Ivanova N., 2015, MNRAS, 449, 4415
Piersanti L., Gagliardi S., Iben I. J., Tornambé A., 2003a, ApJ, 583, 885
Piersanti L., Gagliardi S., Iben I. J., Tornambé A., 2003b, ApJ, 598, 1229
Piersanti L., Tornambé A., Yungelson L. R., 2014, MNRAS, 445, 3239
Piersanti L., Yungelson L. R., Tornambé A., 2015, MNRAS, 452, 2897
Pols O. R., Schroder K., Hurley J. R., Tout C. A., Eggleton P. P., 1998, MNRAS, 298, 525
Popova E. I., Tutukov A. V., Yungelson L. R., 1982, Ap&SS, 88, 55
Postnov K. A., Yungelson L. R., 2014, Living Rev. Rel., 17, 3
Raskin C., Kasen D., 2013, ApJ, 772, 1
Raskin C., Timmes F. X., Scannapieco E., Diehl S., Fryer C., 2009, MNRAS, 399, L156
Raskin C., Scannapieco E., Fryer C., Rockefeller G., Timmes F. X., 2012, ApJ, 746, 62
Rosswog S., Ramirez-Ruiz E., Hix W. R., 2009a, J. Phys. Conf. Ser., 172, 012036

Rosswog S., Kasen D., Guillochon J., Ramirez-Ruiz E., 2009b, ApJ, 705, L128
Ruiter A. J., Belczynski K., Fryer C., 2009, ApJ, 699, 2026
Ruiter A. J. et al., 2013, MNRAS, 429, 1425
Ruiter A. J., Belczynski K., Sim S. A., Seitenzahl I. R., Kwiatkowski D., 2014, MNRAS, 440, L101
Ruiz-Lapuente P., 2014, New Astron. Rev., 62, 15
Ruiz-Lapuente P., Burkert A., Canal R., 1995, ApJ, 447, L69
Sato Y., Nakasato N., Tanikawa A., Nomoto K., Maeda K., Hachisu I., 2015, ApJ, 807, 105
Sato Y., Nakasato N., Tanikawa A., Nomoto K., Maeda K., Hachisu I., 2016, ApJ, 821, 67
Savonije G. J., de Kool M., van den Heuvel E. P. J., 1986, A&A, 155, 51
Scalzo R. et al., 2014a, MNRAS, 440, 1498
Scalzo R. A., Ruiter A. J., Sim S. A., 2014b, MNRAS, 445, 2535
Schwab J., Shen K. J., Quataert E., Dan M., Rosswog S., 2012, MNRAS, 427, 190
Schwab J., Quataert E., Kasen D., 2016, MNRAS, 463, 3461
Seitenzahl I. R., Meakin C. A., Townsley D. M., Lamb D. Q., Truran J. W., 2009, ApJ, 696, 515
Seitenzahl I. R., Cescutti G., Röpke F. K., Ruiter A. J., Pakmor R., 2013, A&A, 559, L5
Shara M. M., Hurley J. R., 2002, ApJ, 571, 830
Shen K. J., Bildsten L., 2014, ApJ, 785, 61
Shen K. J., Moore K., 2014, ApJ, 797, 46
Shen K. J., Kasen D., Weinberg N. N., Bildsten L., Scannapieco E., 2010, ApJ, 715, 767
Shen K. J., Bildsten L., Kasen D., Quataert E., 2012, ApJ, 748, 35
Shen K. J., Guillochon J., Foley R. J., 2013, ApJ, 770, L35
Shigeyama T., Nomoto K., Yamaoka H., Thielemann F.-K., 1992, ApJ, 386, L13
Sim S. A., Röpke F. K., Hillebrandt W., Kromer M., Pakmor R., Fink M., Ruiter A. J., Seitenzahl I. R., 2010, ApJ, 714, L52
Smith B. D., Wise J. H., O'Shea B. W., Norman M. L., Khochfar S., 2015, MNRAS, 452, 2822
Sparks W. M., Stecher T. P., 1974, ApJ, 188, 149
Stritzinger M., Leibundgut B., Walch S., Contardo G., 2006, A&A, 450, 241
Sweigart A. V., Gross P. G., 1978, ApJS, 36, 405
Taam R. E., 1980, ApJ, 242, 749
Tanikawa A., Nakasato N., Sato Y., Nomoto K., Maeda K., Hachisu I., 2015, ApJ, 807, 40
Tauris T., Dewi J. D. M., 2001, A&A, 369, 170
Toonen S., Nelemans G., Portegies Zwart S., 2012, A&A, 546, A70
Toonen S., Claeys J. S. W., Mennekens N., Ruiter A. J., 2014, A&A, 562, A14
Totani T., Morokuma T., Oda T., Doi M., Yasuda N., 2008, PASJ, 60, 1327
Tout C. A., Aarseth S. J., Pols O. R., Eggleton P. P., 1997, MNRAS, 291, 732
Tutukov A. V., Yungelson L. R., 1979a, in de Loore C., Conti P. S., eds, Mass Loss and Evolution of O-Type Stars. Reidel, Dordrecht, p. 401
Tutukov A. V., Yungelson L. R., 1979b, Acta Astron., 29, 665
Tutukov A. V., Yungelson L. R., 1981, Nauchnye Informatsii, 49, 3
Tutukov A. V., Yungelson L. R., 1994, MNRAS, 268, 871
van Haaften L. M., Nelemans G., Voss R., Toonen S., Portegies Zwart S. F., Yungelson L. R., van der Sluys M. V., 2013, A&A, 552, A69
van Kerkwijk M. H., Chang P., Justham S., 2010, ApJ, 722, L157
van Rossum D. R., Kashyap R., Fisher R., Wollaeger R. T., Garcia-Berro E., Aznar-Siguan G., Ji S., Loren-Aguilar P., 2016, ApJ, 827, 128
Waldman R., Sauer D., Livne E., Perets H., Glasner A., Mazzali P., Truran J. W., Gal-Yam A., 2011, ApJ, 738, 21
Wang B., Chen X., Meng X., Han Z., 2009, ApJ, 701, 1540
Webbink R. F., 1979, in van Horn H.-M., Weidemann V., eds, IAU Colloq. 53: White Dwarfs and Variable Degenerate Stars. Rochester University, p. 426
Webbink R. F., 1984, ApJ, 277, 355
Woods T. E., Ivanova N., 2011, ApJ, 739, L48
Yamaguchi H. et al., 2015, ApJ, 801, L31
Yu S., Jeffery C. S., 2010, A&A, 521, 85
Yungelson L. R., 2008, Astron. Lett., 34, 620
Yungelson L. R., Livio M., 2000, ApJ, 528, 108
Zahn J.-P., 1975, A&A, 41, 329
Zhu C., Chang P., van Kerkwijk M. H., Wadsley J., 2013, ApJ, 767, 164
Zhu C., Pakmor R., van Kerkwijk M. H., Chang P., 2015, ApJ, 806, L1
Zorotovic M., Schreiber M. R., Gänsicke B. T., Nebot Gómez-Morán A., 2010, A&A, 520, A86

APPENDIX A: SCENARIOS

Below, we show for scenarios 1–8 the initial distributions of the masses of the components of the progenitor systems, the initial relationships between the masses of primaries and the separation of the components in these systems, and the location of the components of merging systems in the $M_{\rm acc}$–$M_{\rm don}$ diagram. Labels in the figures correspond to Table 1. In Tables A1–A8 we present for each scenario typical tracks leading to merger, indicating evolutionary lifetime (T), evolutionary status of the components (Star1 and Star2), the filling factors of the respective Roche lobes (R1/RL1 and R2/RL2), the masses of the components (M1 and M2) and their separation A (in solar units). If the filling factor is <0.01 we assign to it, for simplicity, the value of 0.0.

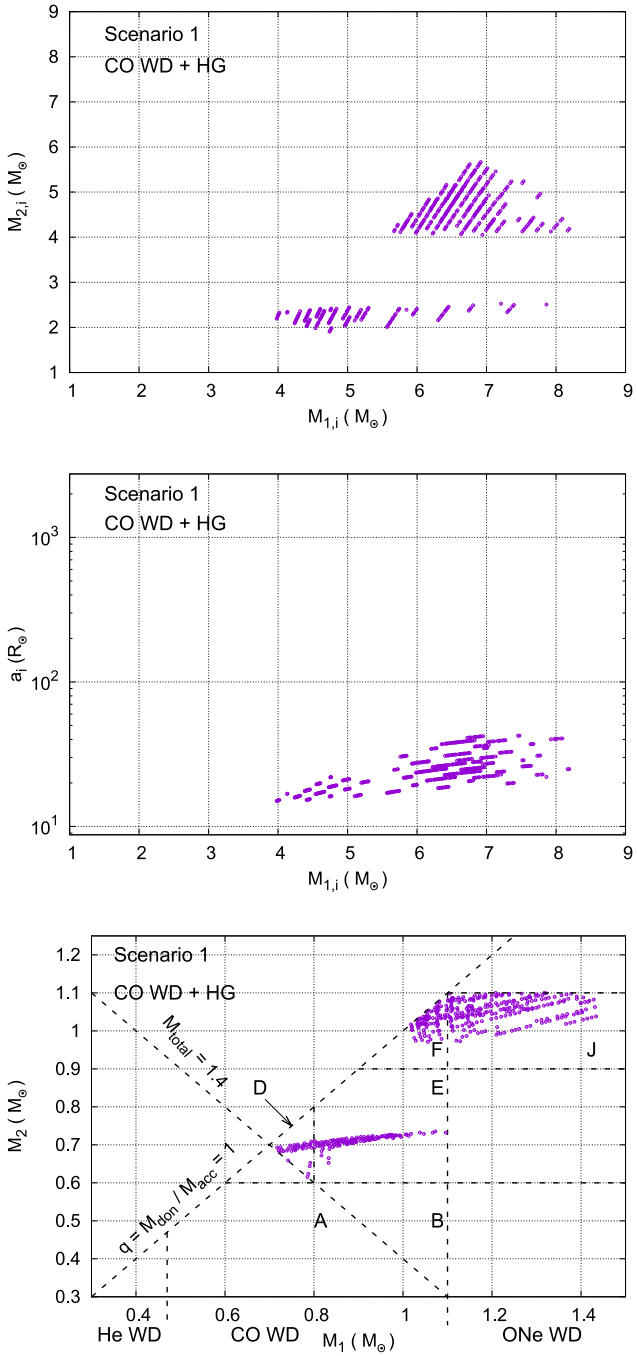

Figure A1. Close binaries evolving via scenario 1. Upper panel: initial distribution of the masses of the components. Middle panel: initial relationship between the masses of primaries and the separation of components. Lower panel: position of merging systems produced via scenario 1 in the $M_{\rm acc}$–$M_{\rm don}$ diagram. The label in the figure indicates the evolutionary stage of the system prior to the first common envelope episode in the system, as in Table 1.

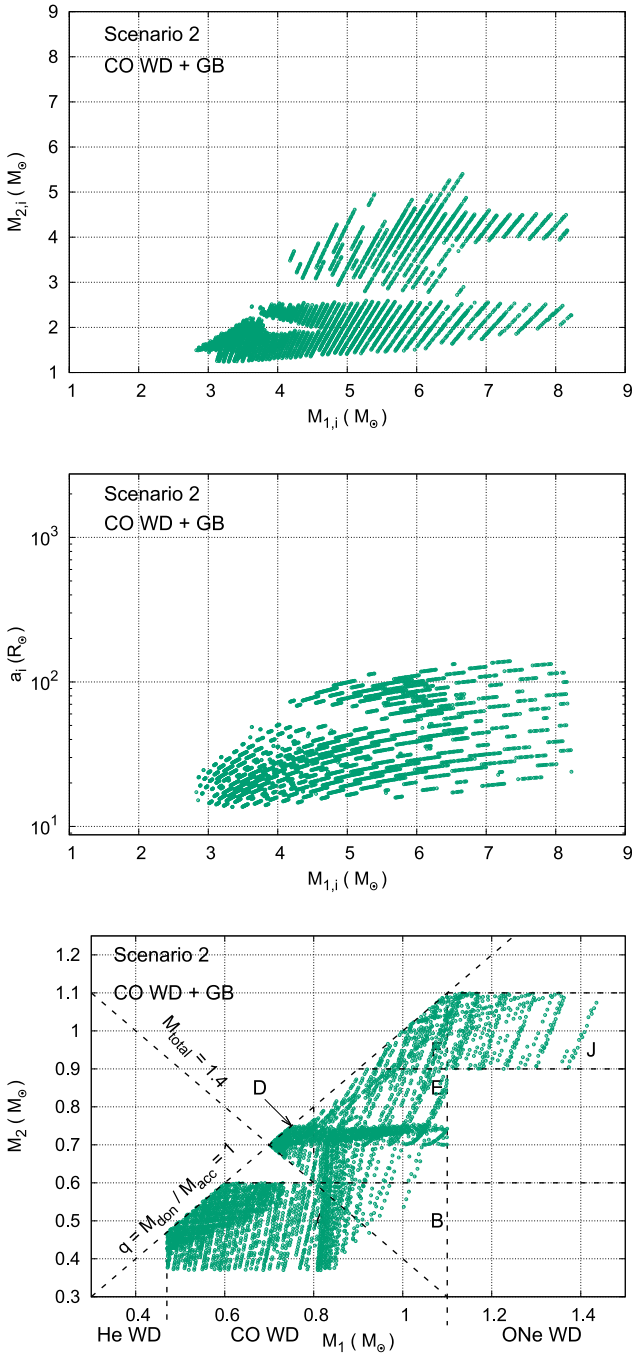

Figure A2. As Fig. A1, but for scenario 2.

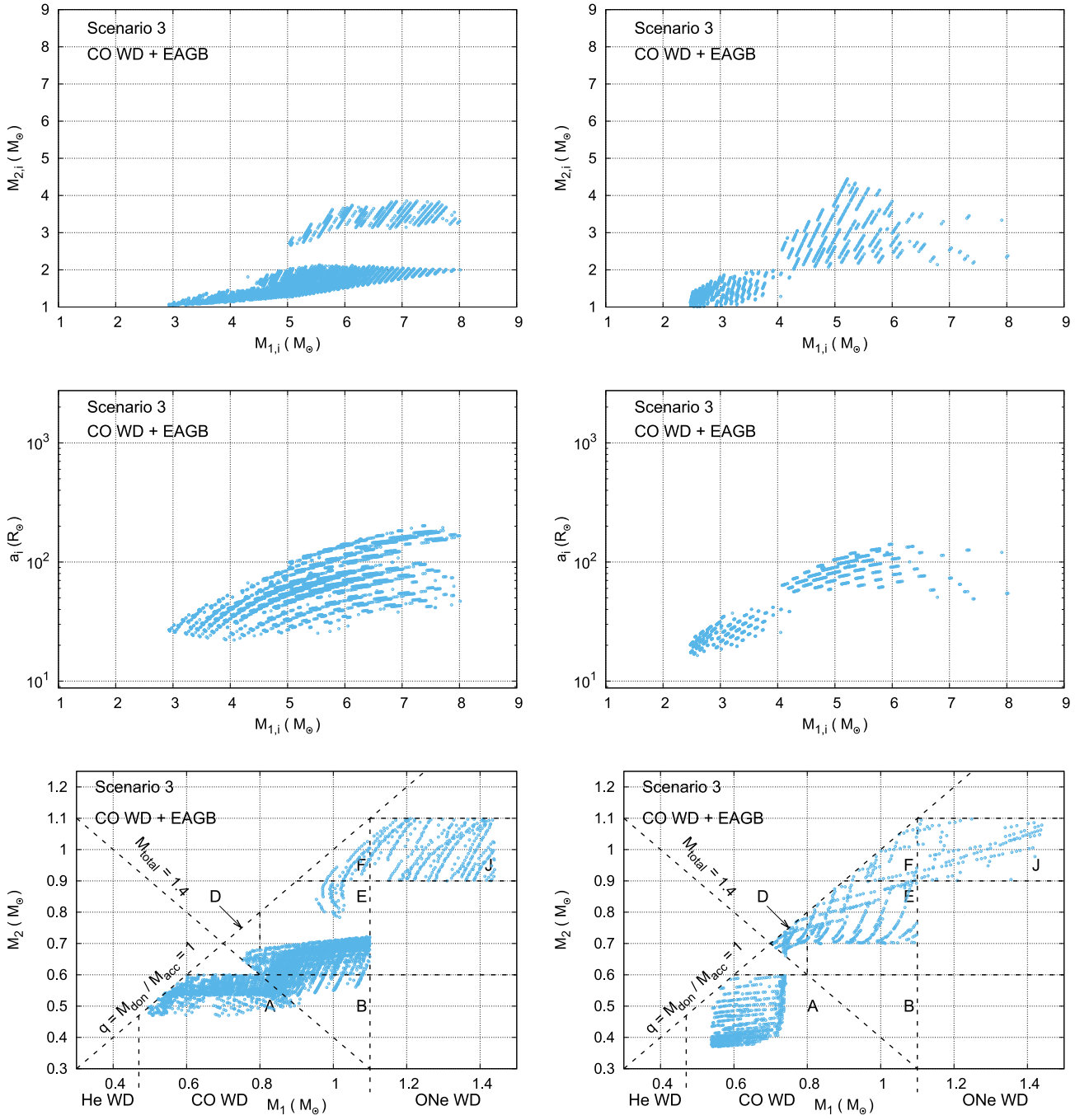

Figure A3. As Fig. A1, but for scenario 3 with $\alpha_{ce}\,\lambda = 0.25$ (left column) and $\alpha_{ce}\,\lambda = 2$ (right column).

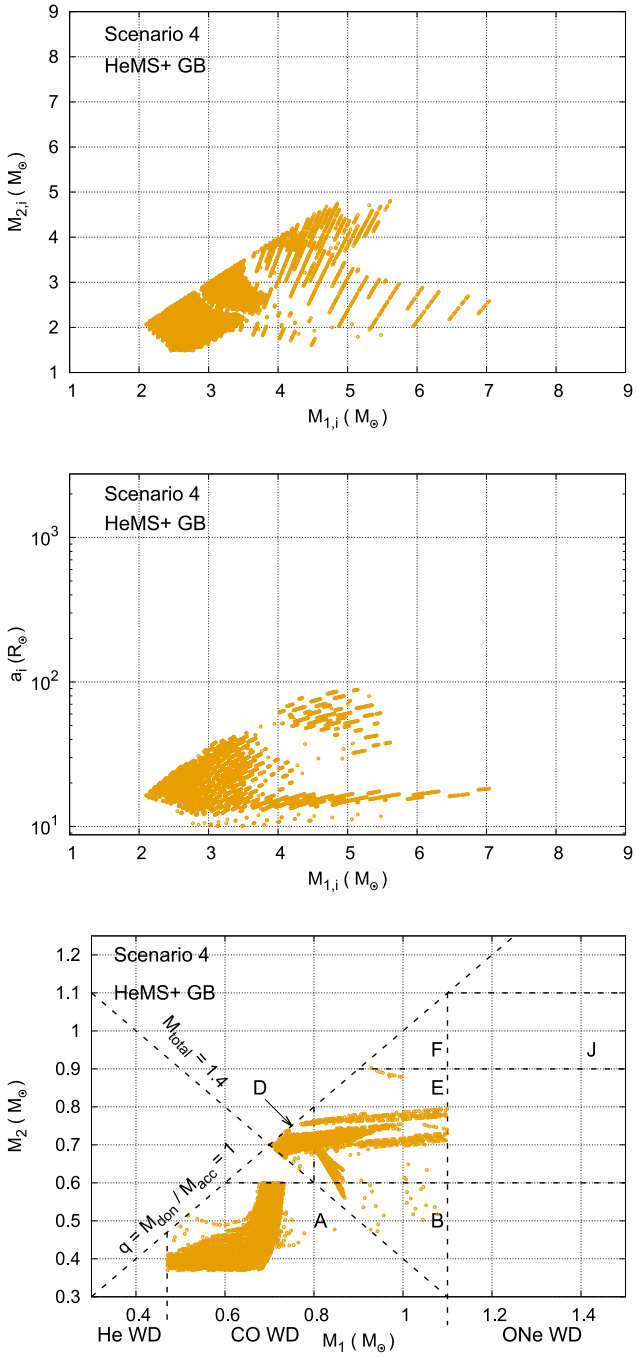

Figure A4. As Fig. A1, but for scenario 4.

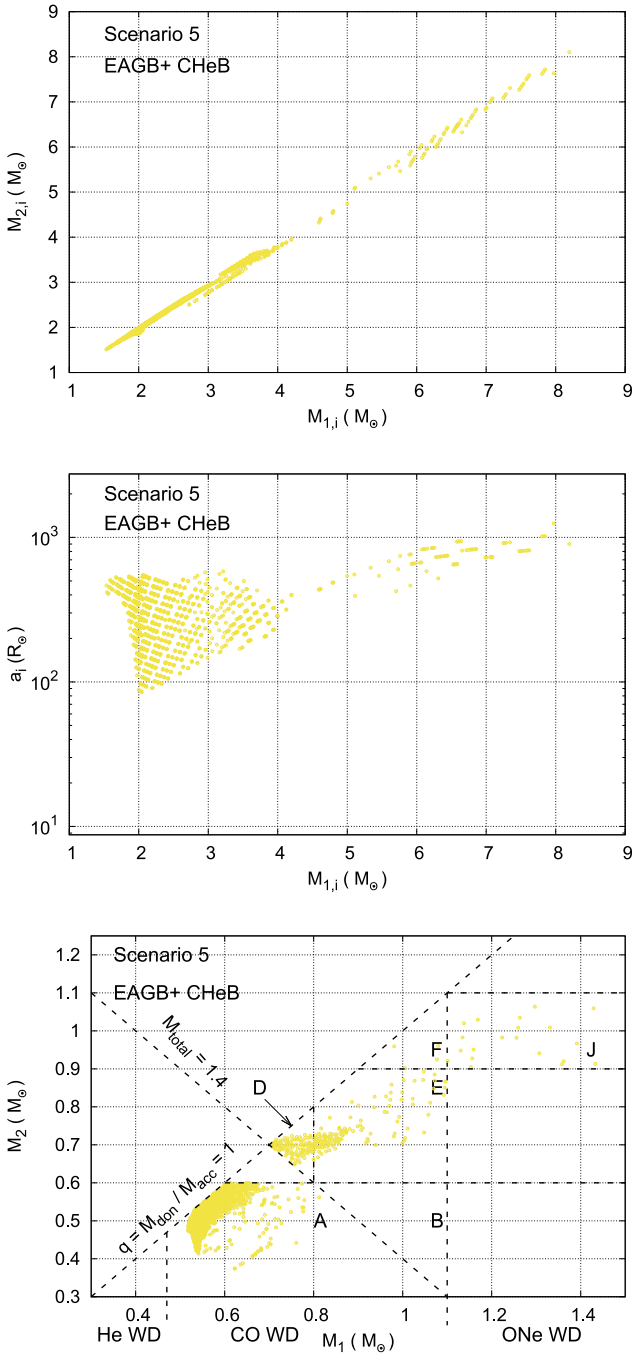

Figure A5. As Fig. A1, but for scenario 5.

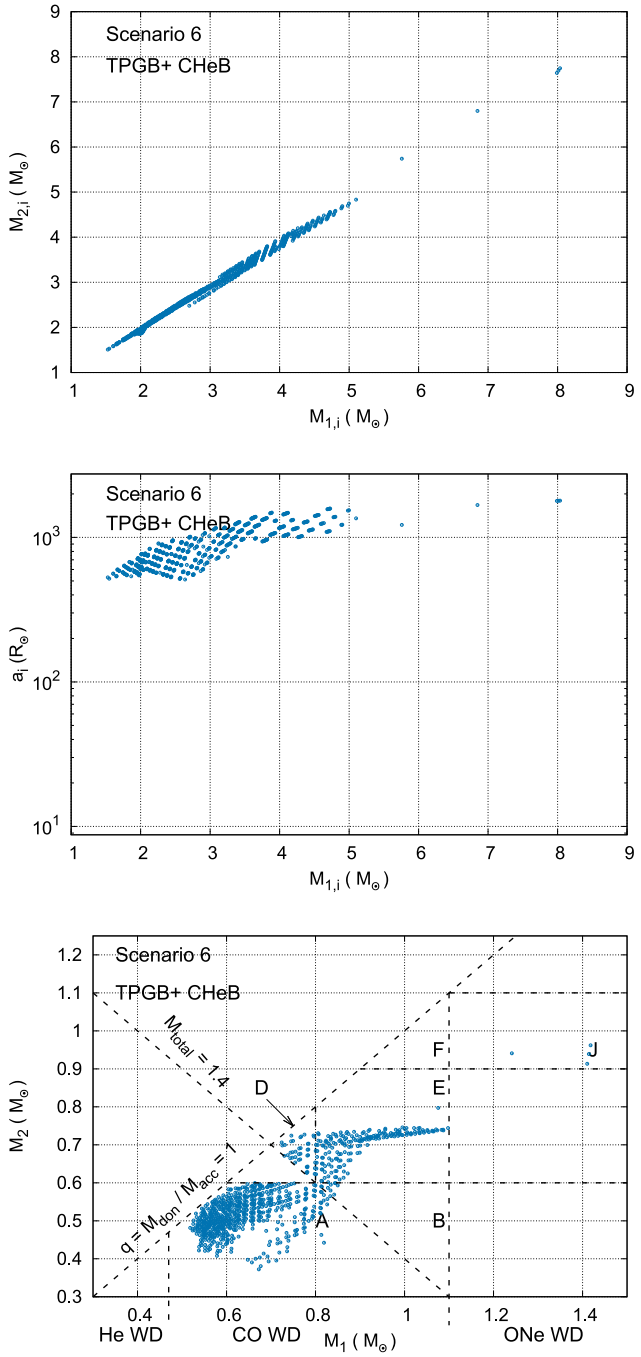

Figure A6. As Fig. A1, but for scenario 6.

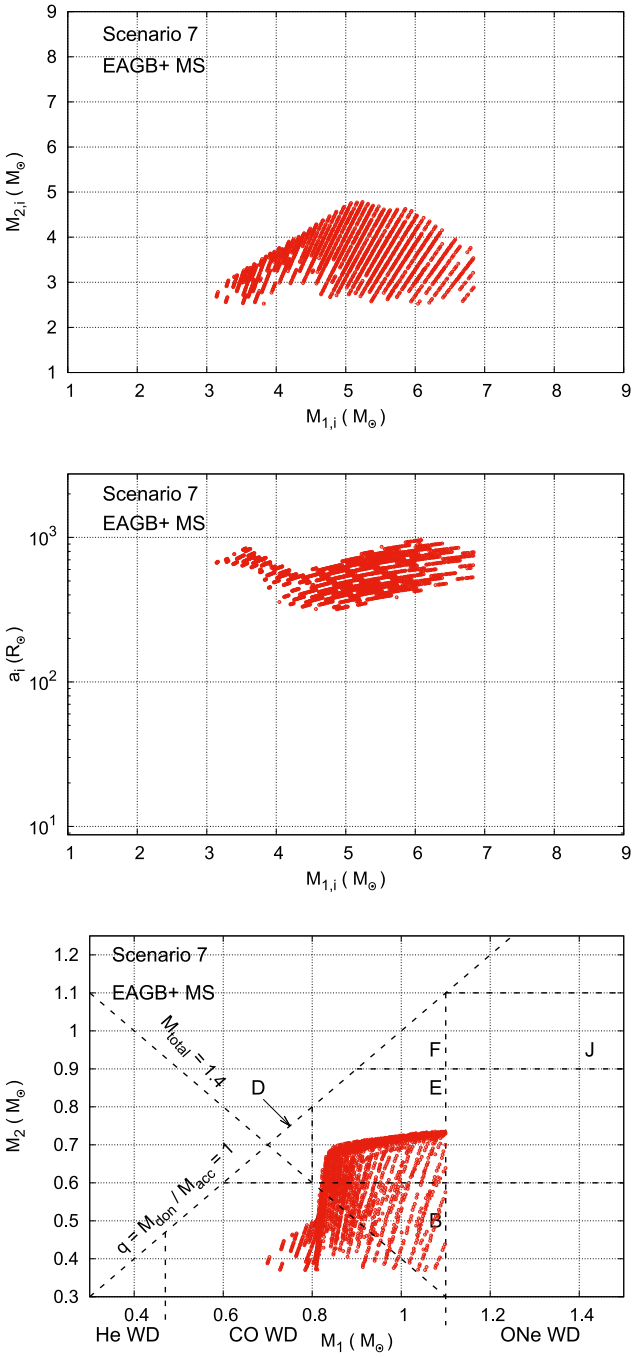

Figure A7. As Fig. A1, but for scenario 7.

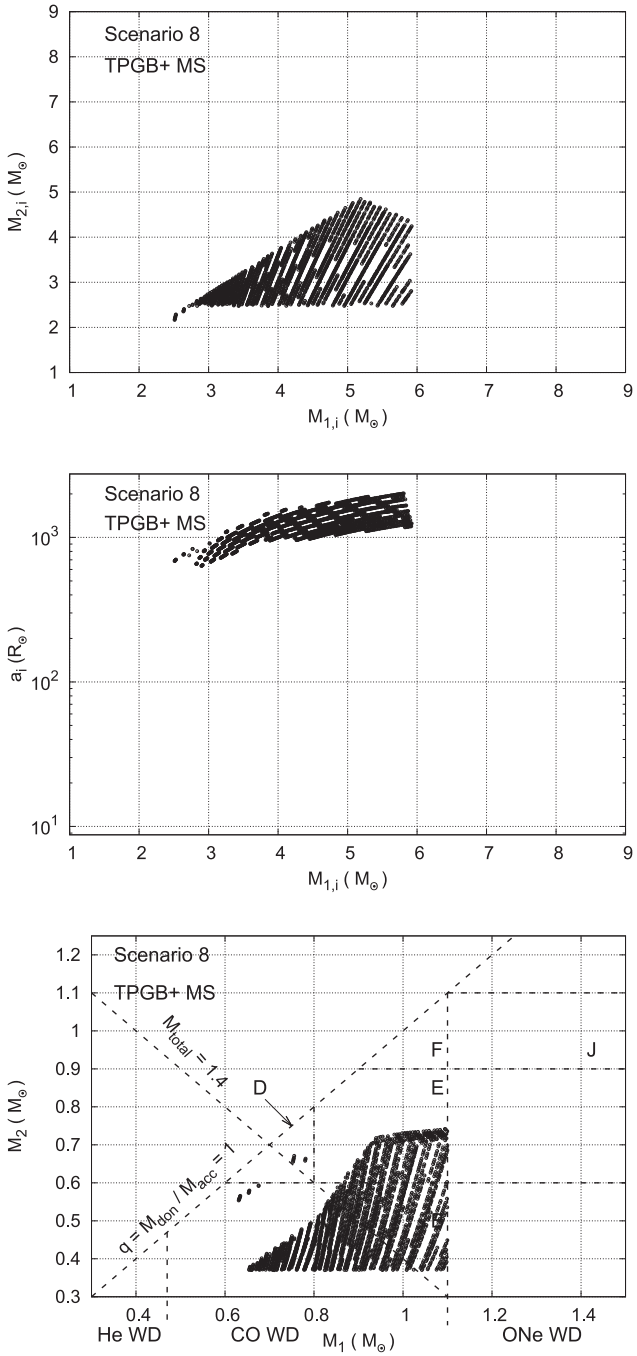

Figure A8. As Fig. A1, but for scenario 8.

Table A1.

Scenario 1: Formation of a CO WD + CO WD pair							
T [Myr]	Star 1	Star 2	R1/RL1	R2/RL2	M1	M2	A
0.0	MS	MS	0.36	0.34	4.42	2.06	15.3
139.8	HG	MS	0.83	0.35	4.42	2.06	15.5
139.9	{ HG	MS	1.00	0.35	4.42	2.06	15.6
140.5	{ GB	MS	1.00	0.09	0.85	4.22	55.5
140.9	HeMS	MS	0.01	0.06	0.72	4.35	72.9
189.4	COHe	MS	0.01	0.08	0.72	4.35	74.0
195.1	COWD	MS	0.001	0.08	0.72	4.35	74.0
276.4	COWD	HG	0.001	0.14	0.72	4.35	74.0
277.1	COWD	HG}	0.001	1.00	0.72	4.35	62.3
			CE				
277.1	COWD	HeMS	0.03	0.39	0.72	0.71	1.06
327.4	COWD	COHe	0.03	0.40	0.72	0.71	1.02
333.2	COWD	COHe}	0.03	1.00	0.72	0.71	1.01
333.3	COWD	COHe	0.03	0.99	0.74	0.69	1.01
333.3	COWD	COWD	0.03	0.03	0.74	0.69	1.01
567.2	COWD	COWD	0.91	1.00	0.74	0.69	0.031
567.2	COWD	COWD	0.91	1.00	0.74	0.69	0.031
567.2	COWD	COWD}	0.91	1.00	0.74	0.69	0.031
			Merger				

Table A2.

Scenario 2.1: Formation of a CO WD + He WD pair							
T ([Myr]	Star 1	Star 2	R1/RL1	R2/RL2	M1	M2	A
0	MS	MS	0.29	0.27	3.79	1.34	16.7
204.9	HG	MS	0.65	0.26	3.79	1.34	17.3
205.2	{ HG	MS	1.00	0.27	3.79	1.34	17.1
206.2	{ GB	MS	1.00	0.06	0.59	2.71	65.0
206.6	HeMS	MS	0.01	0.06	0.59	2.71	65.1
291.5	COHe	MS	0.01	0.06	0.59	2.71	65.7
301.5	COWD	MS	0.00	0.06	0.59	2.71	65.7
687.2	COWD	HG	0.00	0.13	0.59	2.71	65.7
690.3	COWD	GB	0.00	0.35	0.59	2.71	65.8
693.3	COWD	GB}	0.00	1.00	0.59	2.71	48.7
			CE				
693.3	COWD	HeWD	0.03	0.03	0.59	0.40	0.91
1090	COWD	HeWD	0.06	0.08	0.59	0.40	0.57
1165	COWD	HeWD}	0.67	1.00	0.59	0.40	0.05
			Merger				
Scenario 2.2: Formation of a CO WD + CO WD pair							
T (Myr)	Star 1	Star 2	R1/RL1	R2/RL2	M1	M2	A
0	MS	MS	0.20	0.18	4.38	2.34	29
143.4	HG	MS	0.45	0.20	4.38	2.34	29
143.7	{ HG	MS	1.00	0.20	4.38	2.34	29
144.4	{ GB	MS	1.00	0.03	0.72	4.83	155
144.8	HeMS	MS	0.00	0.03	0.72	4.83	156
193.3	COHe	MS	0.00	0.04	0.71	4.83	159
199.1	COWD	MS	0.00	0.04	0.71	4.83	159
246.3	COWD	HG	0.00	0.07	0.71	4.83	159
246.7	COWD	GB	0.00	0.50	0.71	4.83	160
246.9	COWD	GB}	0.01	1.00	0.71	4.83	107
			CE				
246.9	COWD	HeMS	0.02	0.26	0.71	0.82	1.74
281.4	COWD	COHe	0.02	0.25	0.71	0.82	1.76
285.2	COWD	COHe}	0.02	1.00	0.71	0.82	1.75
285.3	COWD	COWD	0.02	0.02	0.80	0.73	1.75
1972	COWD	COWD	0.88	1.00	0.80	0.73	0.03
			Merger				

Table A3.

Scenario 3.1: Formation of a CO WD + CO WD pair							
T [Myr]	Star 1	Star 2	R1/RL1	R2/RL2	M1	M2	A
0	MS	MS	0.09	0.08	5.00	2.62	70
103.8	HG	MS	0.20	0.09	5.00	2.62	70
104.2	{ HG	MS	1.00	0.09	5.00	2.62	70
104.3	{ GB	MS	1.00	0.05	1.70	4.38	124
104.8	HeMS	MS	0.00	0.02	0.87	5.21	337
134.7	COHe	MS	0.00	0.02	0.86	5.21	344
138.2	{ COHe	MS	1.00	0.02	0.86	5.21	344
138.3	COWD	MS	0.00	0.02	0.86	5.21	345
189.5	COWD	HG	0.00	0.03	0.86	5.21	345
189.9	COWD	GB	0.00	0.28	0.86	5.21	345
190.1	COWD	CHeB	0.00	0.96	0.86	5.21	242
203.7	COWD	EAGB	0.00	0.71	0.86	5.14	246
203.7	COWD	EAGB	0.00	1.00	0.86	5.14	180
			CE1				
203.7	COWD	COHe	0.01	0.23	0.86	1.25	5.04
203.9	COWD	COHe	0.01	1.00	0.86	1.25	5.03
			CE2				
203.9	COWD	COWD	0.02	0.02	0.86	0.75	1.48
956.8	COWD	COWD	0.84	1.00	0.86	0.75	0.03
			Merger				
Scenario 3.2: Formation of a CO WD + CO WD pair							
T [Myr]	Star 1	Star 2	R1/RL1	R2/RL2	M1	M2	A
0	MS	MS	0.18	0.18	2.83	1.52	24
440.7	HG	MS	0.42	0.19	2.83	1.52	25
442.9	{ HG	MS	1.00	0.19	2.83	1.52	24
443.4	{ GB	MS	1.00	0.10	1.04	2.51	40
447.8	HeMS	MS	0.00	0.03	0.43	3.12	153
716.2	COHe	MS	0.00	0.05	0.42	3.12	154
743.1	COWD	MS	0.00	0.06	0.42	3.12	154
757.3	COWD	HG	0.00	0.06	0.42	3.12	154
759.3	COWD	GB	0.00	0.19	0.42	3.12	154
761.4	COWD	CHeB	0.00	0.78	0.42	3.12	115
841.0	COWD	EAGB	0.00	0.51	0.42	3.09	116
841.8	COWD	EAGB	0.00	1.00	0.42	3.09	77
			CE				
841.8	COWD	COHe	0.03	0.30	0.42	0.69	1.65
843.7	COWD	COWD	0.03	0.02	0.42	0.69	1.65
4429	{ COWD	COWD	1.00	0.60	0.42	0.69	0.05
			Merger				

Table A4.

Scenario 4.1: Formation of a CO WD + CO WD pair							
T [Myr]	Star 1	Star 2	R1/RL1	R2/RL2	M1	M2	A
0	MS	MS	0.13	0.13	3.47	2.48	40
257.6	HG	MS	0.31	0.16	3.47	2.48	40
258.8	{ HG	MS	1.00	0.16	3.47	2.48	40
259.0	{ GB	MS	1.00	0.10	1.66	4.05	59
267.6	HeMS	MS	0.00	0.02	0.57	5.14	313
337.6	HeMS	HG	0.00	0.04	0.57	5.14	315
338.0	HeMS	GB	0.00	0.28	0.57	5.14	315
338.2	HeMS	GB	0.00	1.00	0.57	5.14	190
			CE				
338.2	HeMS	HeMS	0.18	0.18	0.57	0.90	2.5
351.4	COHe	HeMS	0.15	0.21	0.57	0.89	2.5
362.8	COWD	HeMS	0.02	0.21	0.57	0.89	2.5
366.1	COWD	COHe	0.02	0.18	0.57	0.88	2.5
369.1	COWD	COHe	0.02	1.00	0.57	0.88	2.5
369.2	COWD	COWD	0.01	0.01	0.71	0.74	2.3
6100	COWD	COWD	1.00	0.95	0.71	0.74	0.03
			Merger				
Scenario 4.2: Formation of a CO WD + ONe WD pair							
T (Myr)	Star 1	Star 2	R1/RL1	R2/RL2	M1	M2	A
0	MS	MS	0.12	0.11	5.29	4.15	59
91.2	HG	MS	0.27	0.16	5.29	4.15	59
91.4	{ HG	MS	1.00	0.16	5.29	4.15	59
91.5	{ GB	MS	1.00	0.06	2.06	7.38	123
92.0	HeMS	MS	0.00	0.02	0.93	8.50	449
115.6	HeMS	HG	0.00	0.03	0.92	8.45	462
115.6	HeMS	GB	0.00	0.53	0.92	8.44	463
115.7	HeMS	GB	0.00	1.00	0.92	8.44	341
			CE1				
116.7	COHe	HeMS	0.11	0.14	0.92	1.74	5.5
119.4	{ COHe	HeMS	1.00	0.15	0.92	1.72	5.6
119.5	COHe	HeMS	0.80	0.12	0.78	1.86	6.7
119.5	COWD	HeMS	0.01	0.12	0.78	1.86	6.7
121.5	COWD	COHe	0.01	0.10	0.78	1.82	6.9
122.0	COWD	COHe	0.01	1.00	0.78	1.82	7.0
			CE2				
122.0	COWD	ONeWD	0.02	0.01	0.78	1.04	1.44
592	{ COWD	ONeWD	1.00	0.63	0.78	1.04	0.03
			Merger				

Table A5.

Scenario 5: Formation of a CO WD + CO WD pair							
T [Myr]	Star 1	Star 2	R1/RL1	R2/RL2	M1	M2	A
0	MS	MS	0.03	0.03	2.30	2.29	177
785	HG	MS	0.06	0.07	2.30	2.29	177
791	GB	MS	0.12	0.07	2.30	2.29	177
793	GB	HG	0.14	0.06	2.30	2.29	177
799	GB	GB	0.39	0.12	2.30	2.29	175
800	CHeB	GB	0.48	0.12	2.30	2.29	174
808	CHeB	CHeB	0.18	0.49	2.29	2.29	172
1011	EAGB	CHeB	0.33	0.29	2.27	2.27	177
1014	{ EAGB	CHeB	1.00	0.32	2.27	2.27	168
			CE				
1016	COWD	HeMS	0.03	0.28	0.57	0.56	1.24
1105	COWD	COHe	0.03	0.27	0.57	0.55	1.22
1117	COWD	COWD	0.03	0.03	0.57	0.55	1.22
2121	COWD	COWD	0.98	1.00	0.57	0.55	0.04
			Merger				

Table A6.

Scenario 6: Formation of a CO WD + CO WD pair							
T [Myr]	Star 1	Star 2	R1/RL1	R2/RL2	M1	M2	A
0	MS	MS	0.00	0.00	3.60	3.38	1351
234.3	HG	MS	0.01	0.01	3.60	3.38	1351
235.5	GB	MS	0.04	0.01	3.60	3.38	1351
236.6	CHeB	MS	0.12	0.01	3.60	3.38	1352
275.4	CHeB	HG	0.06	0.01	3.57	3.38	1365
276.9	CHeB	GB	0.06	0.04	3.57	3.38	1366
278.3	CHeB	CHeB	0.07	0.11	3.57	3.38	1367
283.8	EAGB	CHeB	0.08	0.05	3.57	3.37	1375
285.8	TPAGB	CHeB	0.66	0.05	3.53	3.38	1359
286.3	{ TPAGB	CHeB	1.00	0.05	3.34	3.41	1362
			CE				
286.3	COWD	HeMS	0.02	0.36	0.81	0.55	1.02
387.5	COWD	COHe	0.03	0.39	0.81	0.55	0.91
400.0	COWD	COWD	0.03	0.04	0.81	0.55	0.89
567.6	COWD	COWD}	0.63	1.00	0.81	0.55	0.04
			Merger				

Table A7.

Scenario 7: Formation of a CO WD + CO WD pair							
T [Myr]	Star 1	Star 2	R1/RL1	R2/RL2	M1	M2	A
0	MS	MS	0.02	0.01	4.86	4.08	449
111.3	HG	MS	0.03	0.02	4.86	4.08	449
111.7	GB	MS	0.25	0.02	4.86	4.08	449
112.0	CHeB	MS	0.64	0.02	4.86	4.08	437
128.9	EAGB	MS	0.46	0.03	4.80	4.08	444
129.5	{ EAGB	MS	1.00	0.03	4.79	4.08	426
			CE1				
129.5	COHe	MS	0.42	0.20	1.15	4.08	41
129.5	COHe	MS	1.00	0.20	1.15	4.08	41
129.6	COWD	MS	0.00	0.12	0.86	4.37	64
171.3	COWD	HG	0.00	0.17	0.86	4.37	64
171.9	COWD	HG}	0.00	1.00	0.86	4.37	60
			CE2				
171.9	COWD	HeMS	0.02	0.37	0.86	0.72	1.18
221.5	COWD	COHe	0.02	0.38	0.86	0.71	1.14
227.2	COWD	COHe}	0.02	1.00	0.86	0.71	1.13
227.3	COWD	COWD	0.02	0.03	0.88	0.69	1.15
518.6	COWD	COWD}	0.73	1.00	0.88	0.69	0.03
			Merger				

Table A8.

Scenario 8.1: Formation of a CO WD + CO WD pair							
T [Myr]	Star 1	Star 2	R1/RL1	R2/RL2	M1	M2	A
0	MS	MS	0.01	0.01	3.97	3.30	1198
182.4	HG	MS	0.01	0.01	3.97	3.30	1198
183.3	GB	MS	0.06	0.01	3.97	3.30	1198
184.0	CHeB	MS	0.16	0.01	3.97	3.30	1198
217.2	EAGB	MS	0.11	0.01	3.93	3.30	1216
218.7	TPAGB	MS	0.76	0.01	3.89	3.31	1177
219.0	{ TPAGB	MS	1.00	0.01	3.80	3.32	1158
			CE1				
219.0	COWD	MS	0.00	0.07	0.85	3.32	104
291.7	COWD	HG	0.00	0.09	0.85	3.32	104
293.3	COWD	GB	0.00	0.36	0.85	3.32	104
294.6	COWD	GB	0.00	1.00	0.85	3.32	80
			CE2				
294.6	COWD	HeMS	0.01	0.19	0.85	0.51	1.8
436.4	COWD	COHe	0.01	0.19	0.85	0.50	1.8
452.4	COWD	COWD	0.01	0.02	0.85	0.50	1.8
3288	COWD	COWD	0.54	1.00	0.85	0.50	0.04
			Merger				
Scenario 8.2: Formation of a CO WD + CO WD pair							
T [Myr]	Star 1	Star 2	R1/RL1	R2/RL2	M1	M2	A
0	MS	MS	0.01	0.01	3.26	2.94	1093
303.5	HG	MS	0.01	0.01	3.26	2.94	1093
305.2	GB	MS	0.04	0.01	3.26	2.94	1093
306.9	CHeB	MS	0.13	0.01	3.26	2.94	1094
374.7	EAGB	MS	0.08	0.01	3.23	2.94	1108
377.3	TPAGB	MS	0.64	0.01	3.20	2.95	1094
377.9	{ TPAGB	MS	1.00	0.01	3.04	2.97	1097
			CE1				
377.9	COWD	MS	0.00	0.08	0.75	2.97	120
396.6	COWD	HG	0.00	0.08	0.75	2.97	120
398.9	COWD	GB	0.00	0.24	0.75	2.97	120
401.5	COWD	CHeB	0.00	0.98	0.75	2.97	93.5
495.7	COWD	EAGB	0.00	0.64	0.76	2.95	94.5
496.6	COWD	EAGB	0.00	1.00	0.76	2.94	76.5
			CE2				
496.6	COWD	COHe	0.01	0.19	0.76	0.67	2.8
498.8	COWD	COWD	0.01	0.01	0.76	0.67	2.8
13225	COWD	COWD	0.86	1.00	0.76	0.67	0.03
			Merger				

This paper has been typeset from a TEX/LATEX file prepared by the author.